

**STUDY ON VIBRATIONS TRANSMITTED TO PAVEMENTS
DURING WARM-UP PERIOD OF AIRPLANES.**

By
R K Bernhard
Special Consultant, Soil Mechanics Laboratory
Princeton University

For
Airport Development Division
Technical Development Service

Technical Development Note No 48
August 1947



**U S DEPARTMENT OF COMMERCE
CIVIL AERONAUTICS ADMINISTRATION
WASHINGTON, D C**

UNITED STATES DEPARTMENT OF COMMERCE

W AVERELL HARRIMAN, *Secretary*

CIVIL AERONAUTICS ADMINISTRATION

THEODORE P WRIGHT, *Administrator*

C INFORMATION
A AND STATISTICS

CONTENTS

	Page
SUMMARY .	1
INTRODUCTION	1
DESCRIPTION OF INSTRUMENTATION DEVELOPED	4
EXPERIMENTS WITH THE INSTRUMENTS DEVELOPED .	9
RESULTS OF FIELD DEMONSTRATIONS .	12
CONCLUSIONS	13
ACKNOWLEDGEMENTS	14
APPENDIX	15

FIGURE INDEX

Figure

1	Response Curves for Instruments with Two Reference Points (Half Aperiodic Damping)	19
2	Response Curves for Instruments with One Reference Point (Half Aperiodic Damping)	19
3	Phase Angle Versus Discord for Half Aperiodic Damping	20
4.	Diagram of Displacement Indicator with Two Reference Points	21
5	Displacement Indicator with Two Reference Points	22
6	Displacement Indicator with Two Reference Points Holding Down Device and Windshield Removed	23
7	Auxiliary Equipment for Pick-Up Units (Light Shield between Camera and Oscillograph Removed)	24
8	Wiring Diagram of Strain Gage Carrier	25
9	Strain Gage Carrier for Displacement Indicator with Two Reference Points	26
10	Determination of Natural Frequency of Displacement Indicator with Two Reference Points (Strain Gage Carrier Alone) Record of Dying-Out Motion	27
11	Diagram of Displacement Indicator with One Reference Point	28
12	Displacement Indicator with One Reference Point Set-Up for Vertical Motion	29
13	Displacement Indicator with One Reference Point Set-Up for Horizontal Motion	29
14	Determination of Natural Frequency and Damping of Displacement Indicator with One Reference Point Record of Dying-Out Motion	30
15	Amplifier Unit for Displacement Indicators Wiring Diagram	31
16	Static Calibration of Airplane Tire in 400,000 lb Universal Testing Machine	32
17	Static Deflection-Load Diagram of Airplane Tires Air Pressure 30 lb per sq in	33
18.	Imprint of Airplane Tire under a Static Load of 2000 lb Air Pressure 30 lb per sq in Contact Pressure 36 lb per sq in (Heavy Line Squares Represent 1 sq in)	34

Figure	Page
19 Calibration of Displacement Indicator with Two Reference Points Record of Sinusoidal Motion of Vibration Table	35
20 Calibration of Displacement Indicator with Two Reference Points Record of Sinusoidal Motion of Vibration Table	35
21. Calibration of Displacement Indicator with Two Reference Points Record of Sinusoidal Motion of Vibration Table	36
22 Calibration of Displacement Indicator with One Reference Point Record of Sinusoidal Motion of Vibration Table	36
23 Calibration of Displacement Indicator with One Reference Point Record of Sinusoidal Motion of Vibration Table	37
24 Calibration of Displacement Indicators Frequency Spectrum of Vibration Table from 7 to 60 c.p s . .	38
25 Calibration of Displacement Indicators Sinusoidal Motion of Vibration Table Recorded Simultaneously with Both Instruments by Means of an Electronic Switch	39
26 Calibration of Displacement Indicators Record of Hysteresis Loop of a Rubber Damper X-Axis Effect of Damping Action X-Axis Effect of Elastic Action Phase Angle $14^{\circ} 20'$.	40
27 Calibration of Displacement Indicator with Two Reference Points Record of Nonperiodic Motion of Vibration Table	41
28 Calibration Curves for Displacement Indicator with Two Reference Points	42
29 Calibration Curves for Displacement Indicator with One Reference Point	43
30 Cessna Plane on Apron before the Regional Depot at La Guardia Field (New York, N. Y) Side View	44
31 Cessna Plane on Apron before the Regional Depot at La Guardia Field (New York, N. Y) Rear View	44
32 Indicator with Two Reference Points Connected to Airplane Wheel (Windshield Removed) Side View	45
33 Indicator with Two Reference Points Connected to Airplane Wheel (Windshield Removed). Rear View	45
34 Indicator with Two Reference Points and with One Reference Point (Windshield Removed) Side View	46
35 Indicator with Two Reference Points and with One Reference Point (Windshield Removed) Rear View	46
36 Windshield and Airplane Wheel. Front View	47
37 Windshield and Airplane Wheel. Side View	47
38 Record of Displacement Indicator with Two Reference Points Dying-out Motion between Hub of Airplane Wheel and Pavement Caused by an Intermittent Force Applied at the End of One Wing	48
39 Record of Displacement Indicator with Two Reference Points Motion between Hub of Airplane Wheel and Pavement Frequency Spectrum for Propeller Velocities around 1,000 r p m	49
40 Record of Displacement Indicator with One Reference Point Motion of Pavement	49
41 Hysteresis Loop Exciting Force Versus Deformation for One Complete Cycle	50
42 Relation between Phase Angle (φ) and Form of Hysteresis Loop for Sinusoidal Vibrations	50
43. Relation between Phase Angle (φ) and Force Vector (P)	50

STUDY ON VIBRATIONS TRANSMITTED TO PAVEMENTS
DURING WARM-UP PERIOD OF AIRPLANES

SUMMARY

The development described in this Note was performed as part of a study of the effect of vibrations on airport pavement performance which is being carried out for the Technical Development Service of the Civil Aeronautics Administration by the Soil Mechanics Laboratory of Princeton University. The general scope of this Program and a partial Report on the progress made was presented in the Highway Research Board Proceedings, 1944¹, and the final report on this project is in preparation.

The investigation required the development of instruments to record the dynamic characteristics of the airplane-pavement-soil system. A description is given of simple instruments which were designed and built for the purpose of recording vibratory displacements. Furthermore a method is indicated which permits the determination of the frequency and magnitude of vibratory forces transmitted to the pavement and the motion of the pavement by warming-up airplanes. Finally trial field experiments with a Cessna airplane are described which demonstrated the suitability of the instrumentation developed so far.

A few results are presented which were gained from the trial experiments and which refer to the static and dynamic forces transmitted to the pavement and the motion of the pavement during the warm-up period of the airplane.

INTRODUCTION

A Purpose of the Investigation

- 1 To develop instrumentation and procedures for the determination of the frequency and magnitude of vibratory forces transmitted to the airport pavement by an airplane during the period of engine warm-up
- 2 To develop means for measuring the amplitude and frequency of the vibratory motion of the airport pavement during the engine warm-up period
- 3 To determine the suitability of the developed instrumentation by means of field tests employing an airplane
- 4 To obtain from these first trial tests some data on the magnitude and frequency of the vibratory forces transmitted to the pavement by an airplane during warm-up

The above purposes have been achieved and are described in this paper.

B Method of Instrumentation

In order to achieve the first purpose of the investigation, as listed above, the following method was selected

¹"Effect of Vibrations on the Bearing Properties of Soils", by G. P. Tschebotarioff. Proceedings, Highway Research Board, Vol. 24, 1944. Pp. 405-425.

(a) An instrument was designed and was built permitting the projection on the screen of a Cathode-Ray Oscillograph of the vibratory motion of the wheel hub of a warming-up airplane with respect to the adjoining pavement surface. This instrument is subsequently referred to in this Note as "Displacement Indicator with Two Reference Points". It consists essentially of a sample pick-up unit provided with a lucite cantilever equipped with SR-4 strain gages.

(b) A movie-camera was adapted to record the above vibratory motion (a) as projected on the oscillograph screen.

(c) The magnitude of the vibratory displacement of the airplane wheel hub with respect to the pavement surface was determined from the movie-camera (b) and from calibration curves obtained during calibration of the instruments on the electro-magnetic vibration table in the laboratory.

(d) The frequency of the relative airplane wheel hub vibration was determined directly from the movie-camera record (b) and a time signal produced by a neon lamp attached to the oscillograph.

(e) The static spring constant of the airplane tire was determined in the laboratory with the same tire and at the same air pressure which was used during the field tests.

(f) The magnitude of the vertical vibratory forces transmitted to the pavement by the wheel of the warming-up airplane was determined from the static tire spring constant (e) and from the magnitude of the displacement amplitude (c) of the airplane wheel hub.

The second purpose of the investigation, as listed above, was achieved in a manner very similar to the one just described, except that a different type of instrument is used.

(a) An instrument was designed and was built permitting the projection on the screen of a Cathode-Ray Oscillograph of the vibratory motion of the pavement surface immediately adjoining the wheel of a warming-up airplane. This instrument was based on the so-called "seismic principle" and is subsequently referred to in this Note as "Displacement Indicator with One Reference Point".

(b), (c) and (d) The techniques of the following three successive steps were identical to the ones just described and listed under the corresponding letters of the preceding description of the "Indicator with Two Reference Points".

In order to protect the Displacement Indicator pick-up units of both types from the propeller draft, a wind shield was required. This shield served simultaneously as the support for a holding down device of the pick-up units.

No specific data were available with respect to magnitude and frequency of the static and dynamic displacements which could be expected. Hence for all instruments an exceptionally wide measuring range was required.

The simplicity of the final set-up selected, as described above, was considered to compensate for the disadvantage that the measurement cannot be made directly under the airplane wheel. The results obtained with this set-up are considered to be accurate enough.

C Disadvantages of other Methods

Other possible methods of measurement have certain disadvantages. For example, pressure cells, first require a hole in the pavement, second, they disturb

the continuity of the pavement, third, their accuracy depends on the centrality of the loads, and, fourth, it is difficult to place a plane in the proper position with respect to the embedded cell. Furthermore, the accuracy of the response to vibratory forces of existing pressure cells has not yet been determined. Weighing devices protruding above the pavement and similar instruments capable of measuring vibratory forces introduce an additional element into the vibrating airplane-pavement-soil system, which may change the dynamic characteristics of the whole system.

D Significance of the Results Obtained

The field measurements performed to date were intended only to demonstrate the suitability of the instrumentation developed. Accordingly, these measurements have been confined so far to one type of plane, a two-motored Cessna plane (Model T 50) with a wing span of approximately 46 feet and a total weight of 5,000 lbs. All field experiments were carried out on the concrete apron before the Regional Depot of the Civil Aeronautics Administration, at La Guardia Field, (New York, N. Y.)

The maximum dynamic forces transmitted through the tires to the pavement did not exceed $\pm 4\%$ of the original static wheel loads during these trial tests. At first glance this may appear to be an insignificantly small value. However, this is not the case.

By means of plunger tests, Professor Tschebotarioff¹ has shown that for certain soils a considerable penetration of the plunger due to dynamic forces may take place at almost any frequency and that the plunger penetrations due to dynamic forces alone may become up to 45 times larger than plunger penetrations caused by equivalent static forces. Further, so far unpublished plunger test results indicated that under certain conditions the effect of dynamic vibratory forces might be still greater.

The above shows that the effects of even rather small vibratory forces are not to be neglected on certain soils. In this connection, further studies appear necessary of the vibrations transmitted to pavements by different types of planes.

The maximum displacement amplitude of the edge of the concrete apron was found to be ± 0.0022 inches. Results of displacement measurement due to causes other than airplanes can be found in the following references:

- 1 "Effect of Vibrations on the Bearing Properties of Soils", by G. P. Tschebotarioff. Proceedings, Highway Research Board, Vol. 24, 1944. Pp. 405-425.
- 2 "Earthquake Investigations in California 1934-1935". Special Publication No. 901, U. S. Printing Office, Washington 1936.
- 3 "Neue Ergebnisse der dynamischen Baugrunduntersuchung", by H. Lorenz, Zeitschrift V. D. I., Vol. 78, No. 12, March 26, 1934, Pp. 379-385.
- 4 "Highway Investigations by Means of Induced Vibrations", by R. K. Bernhard. The Pennsylvania State College Bulletin, Vol. XXVIII, No. 49, October 2, 1939, Pp. 1-28.
- 5 "Die dynamischen Eigenschaften von Strassen", by F. Meister, Strassenbauverlag, Boerner - Halle.
- 6 "Dynamic Testing of Pavement", by G. Pickett, Journal of the American Concrete Institute, Vol. 16, No. 5, April 1945.

¹"Effect of Vibrations on the Bearing Properties of Soils", by G. P. Tschebotarioff. Proceedings, Highway Research Board, Vol. 24, 1944. Pp. 405-425.

- 7 "Dynamische Untersuchung auf Betonfahrbahndecken", by
A Ramspeck, Forschungsarbeiten aus dem Strassenwesen,
Vol 1, 1937
- 8 "Noise Tremor due to Traffic from an Engineers Point
of View", by R K Bernhard, Journal of the Acoustical
Society of America, Vol 12, No 3, January 1941,
Pp 338-347

A discussion of the interaction in the presence of vibrations between different types of pavements and underlying soils is beyond the scope of this Note. Many additional factors are involved in the performance of airport pavements and the importance of these factors has not yet been fully evaluated. Comparative studies of some additional related phenomena are being performed at present by the Princeton Soil Mechanics Laboratory.

DESCRIPTION OF INSTRUMENTATION DEVELOPED

A GENERAL REQUIREMENTS.

In order to decide what instruments can be used during the investigation, the static and dynamic characteristics governing the measuring range of the particular type of instrument have to be established. The measuring range is limited by a lower and an upper frequency. Between these two frequencies correct indications of the instruments with respect to excursion, and phase are to be expected.

Response curves¹ yield the easiest representation of the measuring range and are of the most general character if dimensionless units are plotted on the X- and Y- axis. A short mathematical derivation of the main equations governing these response curves is given in the appendix.

Response curves may indicate the relation between

- 1 Amplification factor (A), i e. the ratio of the dynamic to the static amplitude,
- 2 Damping (β), or the logarithmic damping decrement (δ),
- 3 Phase angle (φ), i e. the lag between exciter and excited vibration,
- 4 Discord or tuning factor (z), i e. the ratio of the exciting frequency (ω_e) to the natural frequency (ω_n)

Fig 1 represents the response curves for instruments with two reference points, Fig 2, with one reference point and Fig 3, gives the corresponding values between discord (z) and phase angle (φ)

Reference points may be defined as points which have the same motion which has to be measured and furthermore are points which can be used to attach parts of the instruments.

All curves for displacement (x), velocity (\dot{x}), acceleration (\ddot{x}), and phase angle (φ) are plotted for half-aperiodic damping ($\beta=\pi$), a damping which yields the widest possible measuring range. Half-aperiodic damping is a damping for which each successive amplitude of the dying-out vibration is reduced to $1/e^\pi = 1/23.16$ of the preceding amplitude.

¹"Determination of the Static and Dynamic Constants by Means of Response Curves", by R K Bernhard, Journal of Applied Physics, Vol 12, No 12, December 1941, Pp 866-874

The measuring range is determined by an amplification factor $A = \text{unity}$ (1) or $A = \text{constant}$

From the seven response curves as shown in Figs 1-3, general requirements referring to instruments can be set up

Displacement Indicators with Two Reference Points

For instruments with two reference points, the following conclusions can be drawn from Fig 1. The horizontal part of the displacement curve (x), representing the measuring range, ($A=1$), is confined to discords (z) from $z=0$ to $z=0.25$. Furthermore the almost straight line relationship between discord and phase angle (ϕ in Fig 3) from $z=0$ to $z=1$ prevents any phase distortion in this range. The vibrating system as a whole, including pick-up and recorder units, as well as each individual part of these units, must have a natural frequency preferably four times as high as the highest frequency to be measured. Consequently such apparatus are based on a high spring constant and may be called superfrequency instruments.

Displacement Indicator with One Reference Point

For instruments with one reference point, the following conclusions can be drawn from Fig 2. The horizontal part of the displacement curve (x), representing the measuring range ($A=1$), is confined to discords from $z=1.8$ to $z=\infty$. Furthermore, the asymptotic approach to the phase angle $\phi=180^\circ$ (Fig 3) from $z=6$ to $z=\infty$ yields an almost constant phase shift. The vibrating system as a whole as well as each individual part must have a natural frequency preferably not higher than $3/5$ of the lowest frequency to be measured. Consequently such instruments are based on the inertia mass of the vibrating system. They have a low spring constant and may be called subfrequency or seismic instruments.

Acceleration Indicator

In case accelerations have to be measured superfrequency instruments are preferable. For discords ranging from $z=0$ to $z=0.5$, the displacement curve (x) in Fig 2 follows approximately the same law as the acceleration curve (x) in the same Fig, i.e. both curves increase parabolically. Hence the upper limit of the measuring range for accelerations is one-half of the natural frequency. Due to the parabolic increase of curve x in Fig 2, mechanical or electrical filters have to be introduced to screen the records against undesirable interference from high frequency accelerations (harmonics)¹

Velocity Indicators

Velocities are proportional to the exciting frequency (ω_e) for discords from $z=2$ to $z=\infty$. The velocity curve (x) in Fig. 2, shows the measuring range. The simplest indicators to record velocities are subfrequency instruments, generally based on a moving coil in a magnetic field¹

B SPECIFIC REQUIREMENTS

In order to simplify the measuring technique the assumption is made that the difference between the static and dynamic spring constants of the airplane tires is small and can be neglected. Hence static and dynamic forces transmitted to the pavement may be determined with sufficient accuracy by measuring the deformation of the tires.

¹ "Mechanical Vibrations", by R. K. Bernhard, Pitman Publishing Corporation, New York 1943.

A large difference in magnitude between the static deformation of the tire (maximum approximately ± 0.75 inches) and the dynamic deformation (maximum displacement amplitude approximately $\pm 6 \times 10^{-2}$ inches) exists. Let us assume that static and dynamic deformations have to be measured simultaneously and that the static deformation can be recorded with a deviation from the zero line equal to 0.75 inches. Consequently this 0.75 inch deviation will be superimposed by a vibratory motion of $\pm 6 \times 10^{-2}$ inches. Any record of $\pm 6 \times 10^{-2}$ inch amplitudes is too small to permit the required evaluation of such details as frequency, wave, shape, phase differences, etc.

Hence an independent measuring technique of static and dynamic phenomena is desirable, a separation which at the same time facilitates the instrumentation.

STATIC FORCES

A redistribution of the static loads on the plane wheels takes place during the warming-up period. This redistribution depends appreciably upon the rotational speed and the pitch of the propellers. The static deformation of the tires, i.e. the change in distance between hub and pavement multiplied with the tire spring constant, yields the static forces transmitted from the plane to the pavement.

The static deformation has been measured by means of a spring mechanism, sandwiched between the hub of the tire and the pavement (Figs 4, 5 and 6). For these tests the strain gage carrier was blocked. Springs of various strength can be enclosed in a cylinder and compressed by a piston. Piston and cylinder are locked by remote control via a self-locking worm and gear drive. This drive is connected to a flexible shaft which is operated manually at the other end by a small crank shaft. The change in position of the piston within the cylinder can be measured by means of divider and scale. These measurements must be made, first, before the motors are running and, second, after the test, i.e. after the system has been locked at the desired rotational speed of the propellers.

It has to be emphasized that this method yields approximate values only. No attempt has been made to improve the method and to record the static forces. A simple slide wire instrument would yield more accurate results.

DYNAMIC FORCES

Receiver unit

The dynamic effects are superimposed on the static forces. Due to the type of excitation the dynamic forces have in general a quasi-periodic characteristic and no significant transient phenomena have to be measured. The image on a standard cathode-ray oscillograph screen appeared adequate. The screen was photographed on a 35 millimeter film moving with a constant speed of approximately 6 in /sec (Fig 7). The camera was kindly loaned by the Physics Department (Rocknak Lab) of Princeton University. The simultaneously recorded image of a neon lamp yielded a continuous time signal of 60 c p s. Unfortunately only a long persistence, green oscillograph screen (Dumont Cathode-Ray Tube type 5 S P 2) was available which explains the fuzzy appearance of some of the records.

Pick-up unit

To determine the dynamic forces transmitted to the pavement, the change in distance (vibratory motion) between the hub of the tire and the pavement was measured. Hence two reference points, one on the hub and a second on the pavement, were available. The pick-up unit was placed under the above mentioned piston-cylinder connection. The pick-up unit responded only when the cylinder-spring connection was locked. A free motion of the piston within the cylinder was necessary in order to prevent an overstress in the pick-up unit in case of large static deformations.

The pick-up unit consists of a cantilevered plate (Figs 8 and 9) equipped with four SR-4 strain gages^{1,2}. Several contact points at the free end of the cantilevered arm are provided for the connection to the hub of the airplane wheel. The outer points yield the highest sensitivity. Since only dynamic phenomena are to be recorded and no long time tests are involved, direct current from dry cell batteries could be used to feed the bridge circuit. The freely vibrating cantilever system has a natural frequency of 85 c p s (Fig 10). The natural frequency is substantially increased as soon as the rigid connection to the airplane hub is locked, so that the ratio of the exciting frequency to the natural frequency is in general below 0.25. The magnitude of the damping is not critical. Hence the vibrating system fulfills the requirements of the above described displacement indicator with two reference points.

An increase of the natural frequency of the free cantilever system, however, is desirable.

MOTION OF THE PAVEMENT

Receiver unit

The receiver unit consists of the same cathode-ray oscillograph and camera as described before (see Fig 7)

Pick-up unit

To determine the motion of the pavement only one reference point is available, i.e. the pavement itself. The pick-up unit consists essentially of the same parts as the indicator with two reference points. However, the cantilever arm is extended and carries adjustable weights on this extension (Figs 11, 12 and 13). The vibrating system has a natural frequency of 7 c p s. (Fig 14). No frequencies below 15 c p s have to be measured. Hence the instrument fulfills the requirements for the above described seismic type (one reference point). The low natural frequency is obtained by increasing the weights up to 2 kilograms and by mounting the SR-4 strain gages on the cantilever arm in a prestressed position (bent downwards). This is necessary in order to prevent an overstress of the gages.

A further reduction of the natural frequency and an increase of the damping is desirable.

SENSITIVITY

The sensitivity of both displacement indicators has to be increased as much as possible. In order to remain below the noise level, i.e. to prevent the recording of induced currents and hum, two steps are necessary. First, all cables, units and connections have to be shielded and grounded very carefully. This is of particular importance since the radio traffic on the airfield causes a substantial amount of disturbance. Second, the mechanical sensitivity of the pick-up units has to be increased, using only as much amplification in the electronic amplifier as is necessary to produce a one inch double amplitude on the oscillograph screen.

¹"SR-4 News Letters Baldwin Southwark Division, Philadelphia, Pa.", May 1944 to August 1945

²"Measurement of Stresses in Rotating Shafts", by W. F. Curtis, Electronics, July 1945, Pp 114-122

Mechanical parts

1. Four SR-4 strain gages are cemented on the cantilever arm, two on top and two on the bottom. Each of the four gages forms one arm of the bridge circuit (see Fig 8) This set-up eliminates all dummy gages and assures simultaneously an automatic temperature compensation

2. One set of two gages in diagonally opposite arms of the bridge circuit is fixed on the upper side of the cantilever arm, the second set on the lower side (see Fig. 9).

3. The cantilever arm is made of lucite with a low modulus of elasticity of only 5×10^7 p s i. and a flexural strength of 18,000 p s i at 77° F. The low modulus of elasticity causes the required large strain in the gages at a small deflection of the lucite arm The lucite (methyl methacrylate resin type H C 202), which is finally selected, is of a special high heat resistance grade with heat distortion temperature of 199° F, and outstanding weathering resistance The lucite is donated by the Plastics Department of the E. I. du Pont de Nemours and Company, Arlington, New Jersey, for which the reporter is greatly indebted. For further protection the complete gage carrier is covered with wax

Electrical parts

4 The cathode-ray oscillograph responds primarily to changes in input voltage. Hence high resistance strain gages (Baldwin Southwark type C 14) are used. Two dry cell batteries of 45 volts each are connected in series

5 The large resistance of the gages combined with the high voltage of the batteries had the further advantage that small changes in resistance due to longer cable connections play a minor role only

6 A one stage amplifier (Fig 15) is sandwiched between bridge circuit output and oscillograph. The controlling potentiometer of the amplifier is equipped with a 5 inch vernier dial, thus allowing a sufficiently reliable calibration of the complete set-up

The amplifier is designed by Professor J. G. Barry, Princeton University

ACCURACY

Both instruments have been calibrated on an electromagnetic vibration table¹

Displacement Indicator with Two Reference Points.

For this displacement unit an accuracy of $\pm 3\%$ has been obtained within a displacement range from 7×10^{-4} to 7×10^{-2} inches and within a frequency range of 6.5 to 200 c p.s. These values are based on a one inch double amplitude on the oscillograph screen By using different contact points the displacement range can be shifted to higher or lower values respectively

¹"Electromagnetic Vibration Table", by R. K. Bernhard and J. G. Barry, submitted with Report No. 6 of Princeton University, School of Engineering, to the Civil Aeronautics Administration of October 15, 1945

Displacement Indicator with One Reference Point

For this displacement unit an accuracy of $\pm 5\%$ has been obtained within a displacement range from 5×10^{-4} to 5×10^{-3} inches. These values are based on a one inch amplitude on the oscillograph screen and two weights, 1 kilogram each, at the outer end of the cantilever arm extension. For frequencies over 20 c p s the amplitude records become unreliable. It is assumed that additional torsional motions distort the readings.

In order to check whether batteries, tubes, gages, amplifiers, etc. are in good working condition, fixed resistances of 5, 10 and 20 Megohms have been used. Corresponding to the specific setting on the amplifier dial one of the fixed resistances is connected in parallel with one of the strain gages. (See Fig 8) A vibrating make and break contact at one end of the fixed resistance produces a square wave on the oscillograph screen. The amplitude of this square wave has to correspond at all times to an accurately predetermined amount. Slight corrections are possible by adjusting the current in the bridge circuit.

The advantages and disadvantages of the above described measuring systems may be summarized as follows:

Advantages

1. No disturbance of the continuity in the supporting pavement.
2. Large measuring range for static and dynamic displacements.
3. No amplitude-modulation or frequency-modulation carrier system required.

Disadvantages

1. Measuring point not directly under the plane wheel.
2. Static and dynamic effects to be measured separately.
3. No record of static effects.
4. Torsional motions not completely eliminated.

EXPERIMENTS WITH THE INSTRUMENTS DEVELOPED

A. FIRST TRIAL IN THE LABORATORY AND CALIBRATION ON THE VIBRATION TABLE

The experiments in the Laboratory have been confined to the determination of the static spring constant of the airplane tires, the contact area of the tires and the calibration of the instruments.

Airplane tires

Two tires have been used in the field (Firestone 24 x 7 5-10 and General 26 x 8 5-10) and the same tires dismounted and tested in the 400,000 lb universal testing machine of the Princeton Materials Testing Laboratory (Fig 16). To simplify the test procedure the load is applied on top of the tires (double compression). Previous experiments performed by the Armour Institute for the Technical Development Service of the Civil Aeronautics Administration have shown that a load applied to the hub of the tire yields approximately the same deformation. Fig 17 represents the vertical deformation of the tires plotted against the applied load. The air pressure in both tires is 30 p s i. The spring constants for a static load of 2,000 lbs corresponding to the static load of the plane, are 1,724 lb/in and 1,470 lb/in respectively.

An imprint of the second tire under a static load of 2,000 lbs is shown in Fig 18. The contact area of the tire has increased to approximately 55 in², hence the unit load between the tire and the pavement is 36 p s i. The large contact area demonstrates the difficulties which arise when pressure cells are being used.

Influence of Fatigue, Temperature and Long Time Tests

To check the influence of fatigue, temperature and long time tests, in particular with respect to the lucite carrier, a complete pick-up unit has been placed in an oven and heated to 130° F for two hours. Thereafter the instrument was vibrated on the vibration table at various frequencies and amplitudes for six hours while cooling down to 40° F.

No difference of the oscillograph record could be detected.

Influence of cable length

Cables of various length up to approximately 50 feet were inserted between pick-up units, oscillograph and battery box. The difference in indication on the screen for various frequencies and amplitudes did not exceed $\pm 1/2\%$, hence can be neglected. The high resistance of the strain gages, as mentioned previously, may have been the main reason for the small effect of changes in outside resistance.

However, the necessity of very carefully shielding and grounding the shields of all cables, connections and auxiliary units cannot be overemphasized.

FREQUENCY RESPONSE

Periodic motion

Both instruments were subjected to sinusoidal motions on the vibration table. The frequency was varied from 6.5 to 200 c p s. Figs 19, 20 and 21 show the records of a sinusoidal vibration at 6.5, 70 and 160 c.p.s. as transmitted by the displacement indicator with two reference points. Figs 22 and 23 represent a similar motion at 6.5 and 70 c p s. as traced by the displacement indicator with one reference point. No significant deviation from the original sinusoidal form and frequency of the exciting motion can be seen on the records. In Fig 19, 21 and 23 a photograph of the oscillograph screen precedes or follows the actual record. The graduation on the screen facilitates the determination of the magnitude of the recorded excursions.

A continuous frequency spectrum from 7 to 60 c p s. of the vibration table¹ as recorded by both instruments is plotted in Fig 24. The X-axis represents the excited frequency, the Y-axis the recorded displacement double amplitude. A close coincidence between the records of both instruments exists. The resonance ranges of the vibration table first at approximately 8.5 c p s. with the springs of the electromagnet in resonance, second at approximately 13.5 c p s. with the main springs of the table in resonance and third, at approximately 25 c p s. with the table platform at resonance (membrane action) are clearly indicated.

Finally, Fig 25 represents a sinusoidal displacement of the vibration table at 50 c p s. and 10^{-3} inch double amplitude as recorded by both instruments. An electronic switch was used to trace the two records simultaneously. No difference in indication is detectable.

¹"Electromagnetic Vibration Table", by R. K. Bernhard and J. G. Barry, submitted with Report No. 6. of Princeton University, School of Engineering, to the Civil Aeronautics Administration of October 15, 1945.

Hysteresis loop

Another type of simultaneous record of both instruments is shown in Fig. 20. The elliptic curve represents the hysteresis loop^{1,2} of a rubber damper. This damper is vibrated on the vibration table. The elastic effect is recorded by one displacement indicator on the Y-axis of the oscillograph, the damping effect is traced by the other displacement indicator on the X-axis of the oscillograph. For further details see the appendix. The importance of these tests lies in the possibility to determine the damping effect of certain parts of the vibrating system airplane-tire-pavement-subsoil

Nonperiodic motion

Fig 27 shows the motion of the vibration table, excited by impulses at irregular time-intervals. The record indicates the steeper wave fronts of the impulses followed by the sinusoidal dying-out motion after each impulse

Calibration curves

The final results of all these tests are summarized in a few calibration curves. Fig 28 shows the calibration curves for the displacement indicator with two reference points and Fig 29 the corresponding calibration curves for the displacement indicator with one reference point. The X-axis represents the position of the potentiometer dial controlling the amplifier. The dial is always adjusted so that one inch double amplitude appears on the screen of the oscillograph. On the Y-axis the double displacement amplitude of the vibration table is plotted. This double amplitude is varied from 7×10^{-4} to 7×10^{-2} inches and measured by means of a micrometer-microscope illuminated by a stroboscope³. Three different curves corresponding to 10, 12.5 and 15 milliamperes in the bridge circuit are plotted.

All calibration tests on the vibration table have shown so far that the excited displacement amplitude is proportional to the amplitude as indicated on the screen.

The presetting of the double amplitude on the screen for a constant value, in this case for one inch, has the following practical advantages

1 The excursions are always large enough to distinguish details of the vibratory motion without further photographic enlargement

2 A photographic negative (transparent) of the oscillograph screen, showing the graduation of the screen in inches with 1/10 inches subdivision (see Figs 19, 21 and 23) allows a direct evaluation of the magnitude of the recorded excursions.

3 Substantially larger amplitudes on the screen combined with high frequencies might result in an under-exposure of the film, substantially smaller amplitudes combined with low frequencies might yield an over-exposure of the film

4 The total number of required families of calibration curves can be reduced considerably by this decrease of unknown variables

¹"Experimentelle Untersuchung von Schwingungsdaempfernden Unterlagen fuer Maschinen", by E. Schmidt, Gesundheitsingenieur, Vol. 46, No. 6, February 10, 1923.

²"A Vibration Investigation", by L. E. Muller, Mechanical Engineering, Vol. 67, No. 11, November 1945, Pp. 723-728.

³"Electromagnetic Vibration Table", by R. K. Bernhard and J. G. Barry, submitted with Report No. 6 of Princeton University, School of Engineering, to the Civil Aeronautics Administration of October 15, 1945.

B FIELD DEMONSTRATION OF SUITABILITY OF THE INSTRUMENTS

Airplanes

Figs 30 and 31 show the Cessna plane (Model T 50) used for the experiments in the field. The two motors (type Jacobs) of the plane have 7 cylinders and 225 h.p each. The total wing span is approximately 46 feet and the total weight 5,000 lbs.

Pavement

The plane was standing on the concrete apron before the Regional Depot of the Civil Aeronautics Administration at La Guardia Field (New York, N Y). Adjacent to the outer edge of the apron was a flexible pavement. The front wheels were standing approximately two feet from the outer edge.

Instruments

Figs 32 and 33 show the indicator for two reference points with the wind shield removed. In Figs. 34 and 35 the corresponding set up for both pick-up units, i.e. the first indicator with two reference points and the second indicator with one reference points are represented.

Windshield

Figs. 36 and 37 show the windshield which protected the pick-up units from the propeller draft. The shield consisted of four steel plates, 1/4" thick, which could be assembled in the field. The assembled shield was rigid and heavy enough not to move under the propeller draft. One of the side walls of the shield served as support for the holding-down device of the pick-up units.

Test procedure

The records were taken for various speeds of the propellers ranging from 600 to 2,000 r.p.m. One or two motors were running, both with low or high pitch of the propeller blades. At most tests the double amplitude on the oscillograph screen was adjusted to approximately one inch.

RESULTS OF FIELD DEMONSTRATIONS

In Figs. 38, 39 and 40 small sections of three characteristic records are reproduced.

Natural frequency of wing

Fig. 38 shows the dying-out motion between hub of airplane wheel and pavement recorded by the displacement indicator with two reference points. The motion was excited by an intermittent force applied manually at the end of one wing.

The dying-out frequency is approximately 20 c.p.s. and corresponds probably to the natural frequency of the excited wing¹.

The maximum force amplitude transmitted via the tire to the pavement amounted to approximately ± 1 lb.

The time signal along the upper edge of this record represents 60 c.p.s.

¹"Measurement and Prediction of Aircraft Vibration", by E. F. Critchlow, S A E Journal, Vol 52, No 8, September 1944. Pp 368-379.

Motion between hub of airplane wheel and pavement

Fig 39 shows the motion between the hub of the airplane wheel and the pavement, recorded by the displacement indicator with two reference points. This motion was traced while the right propeller rotated at approximately 1,000 r p m. at high pitch and the left propeller was idling

The maximum force amplitude transmitted via the tire to the pavement amounted to approximately ± 22 lbs

Two main frequencies are predominant. A low frequency in the range of 3 c p s represents probably the natural frequency of the plane on the tires. A high frequency in the range of 50 c p s. which was transmitted to the pavement, may correspond to the natural frequency of the vibrating system pavement-soil mass

The overlapping parts on the record are due to a small amplitude and low frequency sweep of the cathode-ray. The time signal of this record on the upper edge represents 75 c p s

Motion of the pavement

Fig 40 shows the motion of the pavement recorded by the displacement indicator with one reference point. This motion was traced while the right propeller rotated at 1,200 r.p.m. at high pitch and the left propeller was idling.

The maximum displacement amplitude is ± 0.0022 inches

Two main frequencies are predominant, a medium frequency in the range of 15 c.p.s. and a high frequency in the range of 50 c p s. The low frequency of 3 c.p.s., as recorded in Fig 39, is apparently not transmitted to the pavement. As mentioned before, the high frequency range coincides with the 50 c p s frequency range of the hub-pavement motion

The time signal of this record on the upper edge represents 60 c p s

CONCLUSIONS

Static forces transmitted to the pavement

The redistribution of the static load of 2,000 lbs on each of the front wheels of the plane depends appreciably upon the rotational speed and the pitch of the propellers. The maximum change of the static load amounted to approximately $\pm 1,100$ lbs. Hence the static load may have been reduced to a minimum of + 900 lbs

Dynamic forces transmitted to the pavement

The maximum dynamic forces transmitted through the tires to the pavement amounted to approximately ± 90 lbs. This dynamic load represents $\pm 4.5\%$ (total 9%) of the original static load of 2,000 lbs and $\pm 10\%$ (total 20%) of the minimum static load of + 900 lbs.

The main frequencies observed are in the range of 3 and 50 c p s

Displacement amplitudes of the pavement

The maximum displacement double amplitudes on the pavement surface amounted to approximately 4×10^{-3} inches. These displacements if transmitted to the subsoil are of a ten times larger magnitude than the soil vibrations as mentioned in the

introduction of this report¹ with reference to the Highway Research Board Proceedings 1944

The main frequencies observed are in the range of 15 and 50 c p s

All conclusions are only preliminary, mainly due to the fact that but one series of recorded field tests have been performed so far and that from 100 feet fall records, exposed on these tests, the evaluation of a few sections only could be included in this report

1 The instruments to measure the dynamic characteristics of the pavement under warning-up airplanes seems to yield reliable results. It is understood, however, that further improvements to these instruments are desirable

2 The field tests indicate that vibratory motions transmitted via the plane wheels and the pavement to the subsoil are of such a magnitude that they may cause settlements of any subsoil sensitive to dynamic forces

ACKNOWLEDGMENTS

The development work described in this Note has been performed as part of a contract between Princeton University and the Civil Aeronautics Administration. The support provided to the project by Mr. D. M. Stuart, Director, Technical Development Service, by Mr. Fred H. Griere and Mr. D. S. Jenkins who successively headed the Airport Development Section during the work on the project, and by Mr. George W. McAlpin of the same section of the Civil Aeronautics Administration is hereby acknowledged

Professor K. H. Condit, Dean of the School of Engineering, and Professor Philip Kissam, former Chairman, and Professor E. K. Tinoy, present Chairman, of the Department of Civil Engineering, have supported the development of the project at Princeton University

All investigations on this project are carried out by the Princeton Soil Mechanics Laboratory in the charge of Professor G. P. Tschebotarioff, Director of the Laboratory, whose valuable advice and active participation in the development has been greatly appreciated

Professor J. G. Barry of the Princeton Electrical Engineering Department, who supervised the development of all the electrical equipment, and Mr. E. R. Ward Research Associate of the Princeton Soil Mechanics Laboratory cooperated with the reporter through all phases of the investigation, have contributed considerably to the project

The Engineering Personnel of Region One, Civil Aeronautics Administration has cooperated in the performance of the field experiments at La Guardia Airport, in New York

Mr. H. Ashworth, Instructor at the Princeton Aeronautical Engineering Department, Mr. C. E. Kjetsaa, Instructor at the Princeton Mechanical Engineering Department, and Mr. M. Watson, Technician of the Princeton Electrical Engineering Department, have built and assembled the various units described in this Note

The author of this Note, acting as Consultant, has designed the equipment, and has supervised its assembly, its operation and the experiments

¹"Effect of Vibrations on the Bearing Properties of Soils", by G. P. Tschebotarioff Proceedings, Highway Research Board, Vol. 24, 1944 Pp 405-425

APPENDIX

A few fundamental equations and concepts used in the report will be discussed as follows

1. Response Curves Relative viscous damping can be defined by the equation

$$k = \frac{V_{cm}}{A} \quad (\text{lb in}^{-1}\text{sec}) \quad (1)$$

where A = amplification factor at resonance (Dimensionless)

c = spring constant (lb in^{-1})

and m = mass ($\text{lb in}^{-1}\text{sec}^2$)

For instruments with two reference points, the general equation of the amplification factor (A_x) referring to the excursion (x) is

$$A_x = \frac{1}{\sqrt{(z^2 - 1)^2 + \frac{(zk)^2}{m\omega_n}}} \quad (2)$$

where z = tuning factor = $\frac{\omega_e}{n}$ (dimensionless)

e = exciting frequency (sec^{-1})

and n = natural frequency (sec^{-1})

Equation (1) yields $A_x = 1$ for $z = 0$, and $A_x = 0$ for $z = \infty$ (Fig 1).

Equation (2) is the same as for a "one-mass" system (one degree of freedom), where the mass is excited by a constant force vector

For instruments with one reference point the general equation of the amplification factor (A_{x_1}) referring to the excursion (x_1) is

$$A_{x_1} = \frac{z^2}{\sqrt{(z^2 - 1)^2 + \frac{(zk)^2}{m\omega_n}}} \quad (3)$$

and yields $A_{x_1} = 0$ for $z = 0$, and $A_{x_1} = 1$ for $z = \infty$ (Fig 2)

Equation (3) is the same as for a "one-mass" system (one degree of freedom), where the mass is excited by a force vector increasing with the square of the exciting frequency (ω_e^2)

In case of a sinusoidal motion

$$x = a \sin(\omega_e t) = \text{excursion}$$

$$\dot{x} = a\omega_e \cos(\omega_e t) = \text{velocity}$$

$$\text{and } \ddot{x} = -a\omega_e^2 \sin(\omega_e t) = \text{acceleration}$$

Hence the velocity response curve (\dot{x}) can be obtained by multiplying the corresponding displacement curve (x) with ω_e , and the acceleration curve (\ddot{x}) by multiplying the corresponding velocity curve (\dot{x}) with ω_e^2

TABLE I

Relation between Discord (z) and Displacement (x), Velocity (\dot{x})

Acceleration (\ddot{x}) and Phase Angle (φ) for Half-Aperiodic Damping ($\gamma = \pi$)

where the values A_x refer to instruments with two reference points or constant force amplitudes

the values A_{x_1} refer to instruments with one reference point or force amplitudes increasing with the square of the exciting force

and the values φ refer to both types of instruments or forces

z	ω_e	A_x	$A_x = \omega_e A_x$	$A_x = A_{x_1} = \omega_e^2 A_x$	$A_{x_1} = \omega_e^3 A_x$	$A_{x_1} = \omega_e^4 A_x$	φ
0 0	0 0	1 000	0 000	0 000	0 000	0 0000	0
0.2	0.2	1 000	0 200	0 040	0 008	0 0016	10° 25'
0.4	0.4	0.985	0 394	0 158	0 063	0.025	33° 58'
0 6	0.6	0.940	0.564	0 338	0 203	0.121	52° 58'
0 8	0 8	0 841	0.673	0 538	0 430	0 344	72° 21'
1 0	1.0	0 707	0.707	0 707	0.707	0 707	90°
1 2	1 2	0 571	0 684	0 821	0.985	1 183	107° 33'
1 4	1 4	0 455	0 636	0 890	1 246	1.744	115° 52'
1.6	1.6	0 364	0 566	0 905	1.449	2.320	124° 35'
1 8	1 8	0 295	0 531	0 956	1 752	3 155	131° 21'
2 0	2 0	0 243	0 486	0 972	1.945	3 890	136° 41'
3 0	3 0	0 1104	0 331	0 993	2 980	8.940	152° 04'
4 0	4 0	0.0625	0 250	1.00	4.000	16 000	159° 20'
5.0	5.0	0 0400	0 200	1 00	5 000	25.000	163° 35'
6 0	6 0	0.0278	0 167	1.00	6 000	36.000	166° 22'

□ = measuring ranges

Table I represents the numerical evaluation of equations (2) and (3) for the logarithmic damping decrement $\delta = \pi$,¹²⁾ which is called half aperiodic damping

$$\text{For half aperiodic damping } A = \frac{1}{\sqrt{2}}$$

Hence all six curves, as shown in Fig 1 and 2, pass through the same point with the abscissa $z = 1$ and the ordinate $A = 0.707$

2

a. Phase Angle The combined record of two pickup units on one cathode ray oscillograph is of special importance. Connecting the first pair of plates of the oscillograph with the exciting force measuring unit, i.e. the deformation due to elastic action, and the second pair of plates with the excited force measuring unit, i.e. the deformation due to damping action, yields the so-called hysteresis loop. The area of this loop represents the energy dissipated during one complete cycle and may be used to determine the internal damping. This hysteresis loop for sinusoidal vibrations is plotted in Fig. 41.

The hysteresis ellipse degenerates, depending on the phase angle (φ), into the following forms, as demonstrated in Fig. 42.

a an ellipse with horizontal and vertical principal axis if the phase angle

$$\varphi = \frac{\pi}{2}$$

b a diagonal of the enveloping rectangle if the phase angle $\varphi = 0$ or $= \pi$

and c a straight horizontal line if $P = \text{constant}$

The phase angle (φ), that is the angle indicating the lag of the deformation vector behind the exciting force vector, can be determined from the following equation (see Fig. 43)

$$\varphi = \sin^{-1} \frac{d}{e} \quad (4) \quad 15)$$

where $d =$ half amplitude of deformation due to damping action (in)

and $e =$ half amplitude of deformation due to elastic action (in.)

The general equation for the phase angle is

$$\tan \varphi = \frac{k \omega_e}{c - m \omega_e^2} \quad (5) \quad 11)$$

Substituting in equation (5) for the relative damping $k = \sqrt{cm}$ (equ 1) and for the damping factor at half aperiodic damping $A = \frac{1}{\sqrt{2}}$ yields

$$\varphi = \tan^{-1} \frac{\sqrt{2z}}{1 - z^2} \quad (6)$$

From this equation the values for the phase angle (φ), as shown in Fig 3 and Table I, are computed.

3 Damping An equation for the relative damping (k), in connection with the hysteresis loop, may be derived as follows. For the stable dynamic equilibrium the energy input W_p (for one cycle) due to the exciting force P must be equal to the

energy dissipation W_D (for one cycle) due to the damping force. Assuming arbitrarily that the damping is essentially viscous in character, then for sinusoidal vibrations

$$1 \quad W_P = \int_{\omega_e t = 0}^{\omega_e t = 2\pi} P dx \quad (7)$$

Substituting for $P = P_o \sin(\omega_e t)$ and for $dx = e\omega_e \cos(\omega_e t - \varphi) dt$ yields

$$2 \quad W_P = P_o \sin \varphi \pi \quad (8)$$

$$W_D = \int_{\omega_e t = 0}^{\omega_e t = 2\pi} k x dx \quad (9)$$

Substituting for $x = \frac{dx}{dt} = e\omega_e \cos(\omega_e t - \varphi)$ yields

$$W_D = k e^2 \omega_e \pi \quad (10)$$

From equating (8) to (10) follows

$$k = \frac{P_o}{e\omega_e} \sin \varphi$$

and since $\sin \varphi = \frac{d}{e}$ (equ 4)

Finally

$$k = \frac{P_o}{e^2} \frac{1}{\omega_e} d \text{ (lb in.}^{-1}\text{sec)} \quad (11)$$

where $P_o =$ exciting force vector (lb)

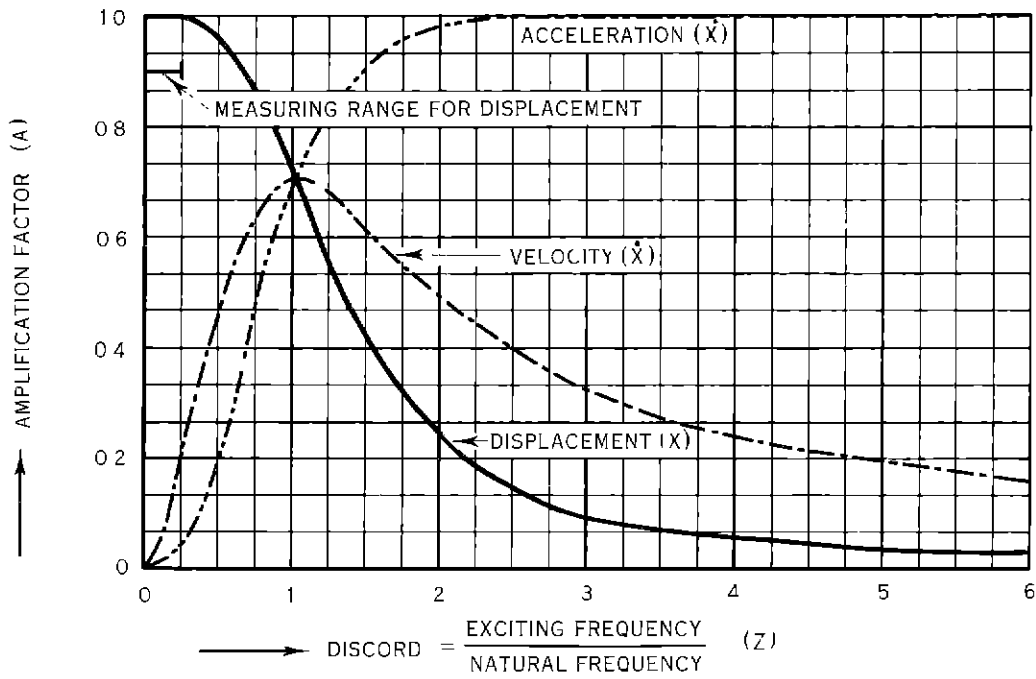


Figure 1 Response Curves for Instruments with Two Reference Points (Half Aperiodic Damping)

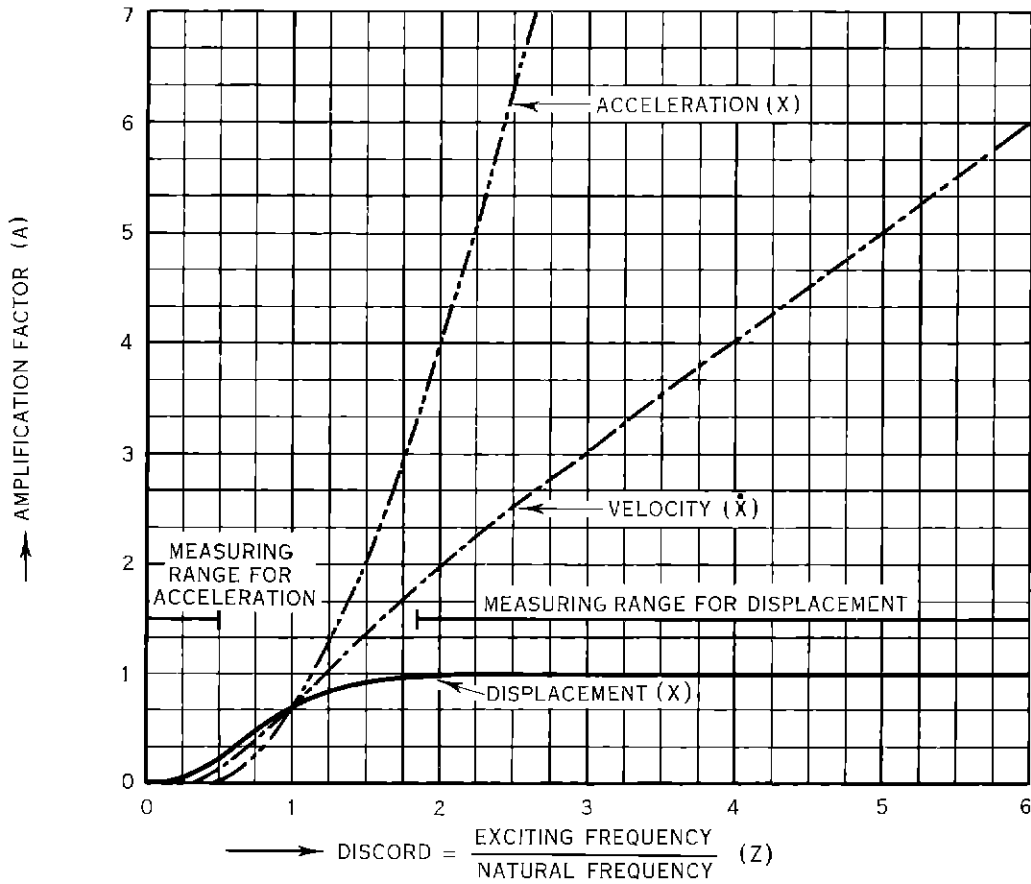


Figure 2 Response Curves for Instruments with One Reference Point (Half Aperiodic Damping)

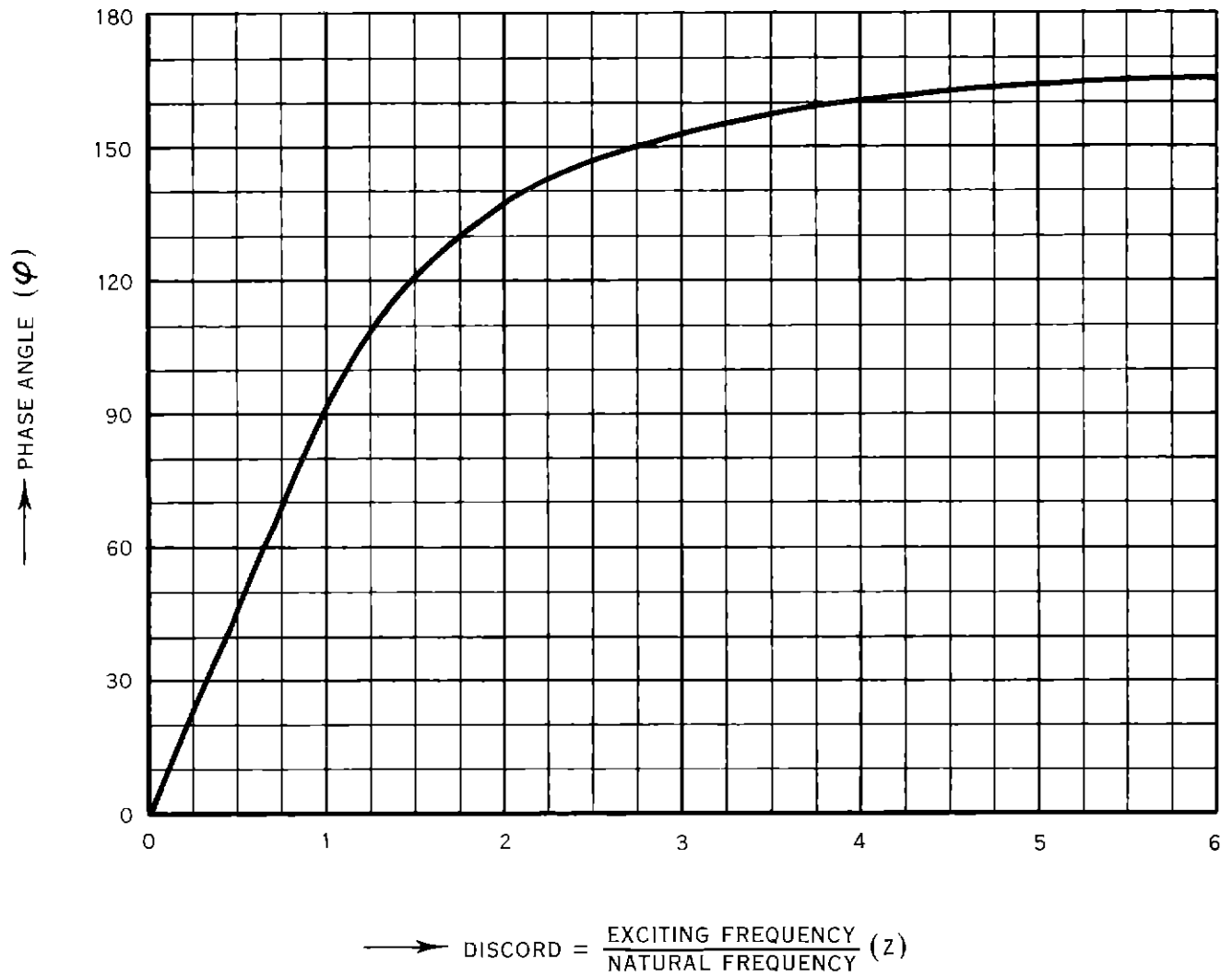
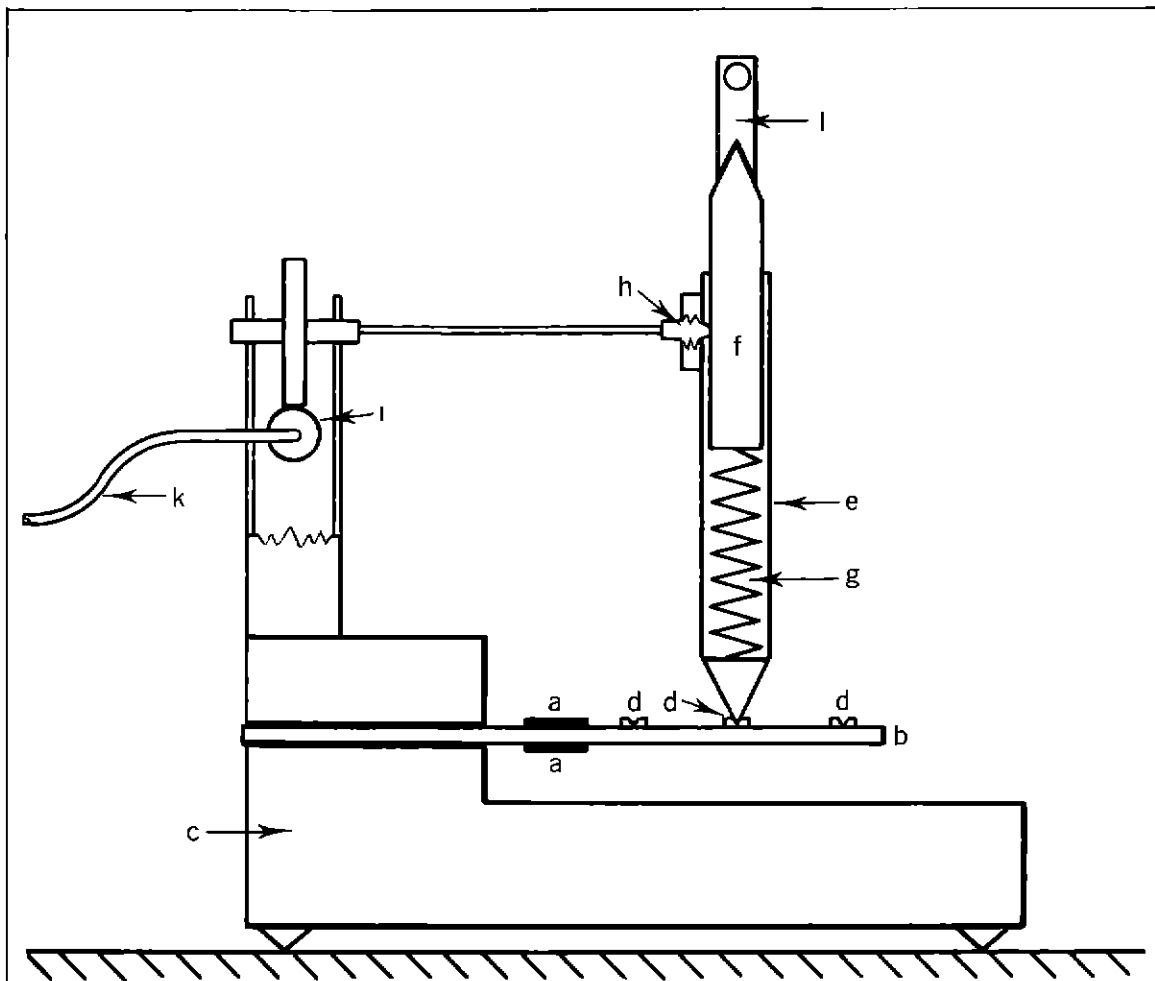
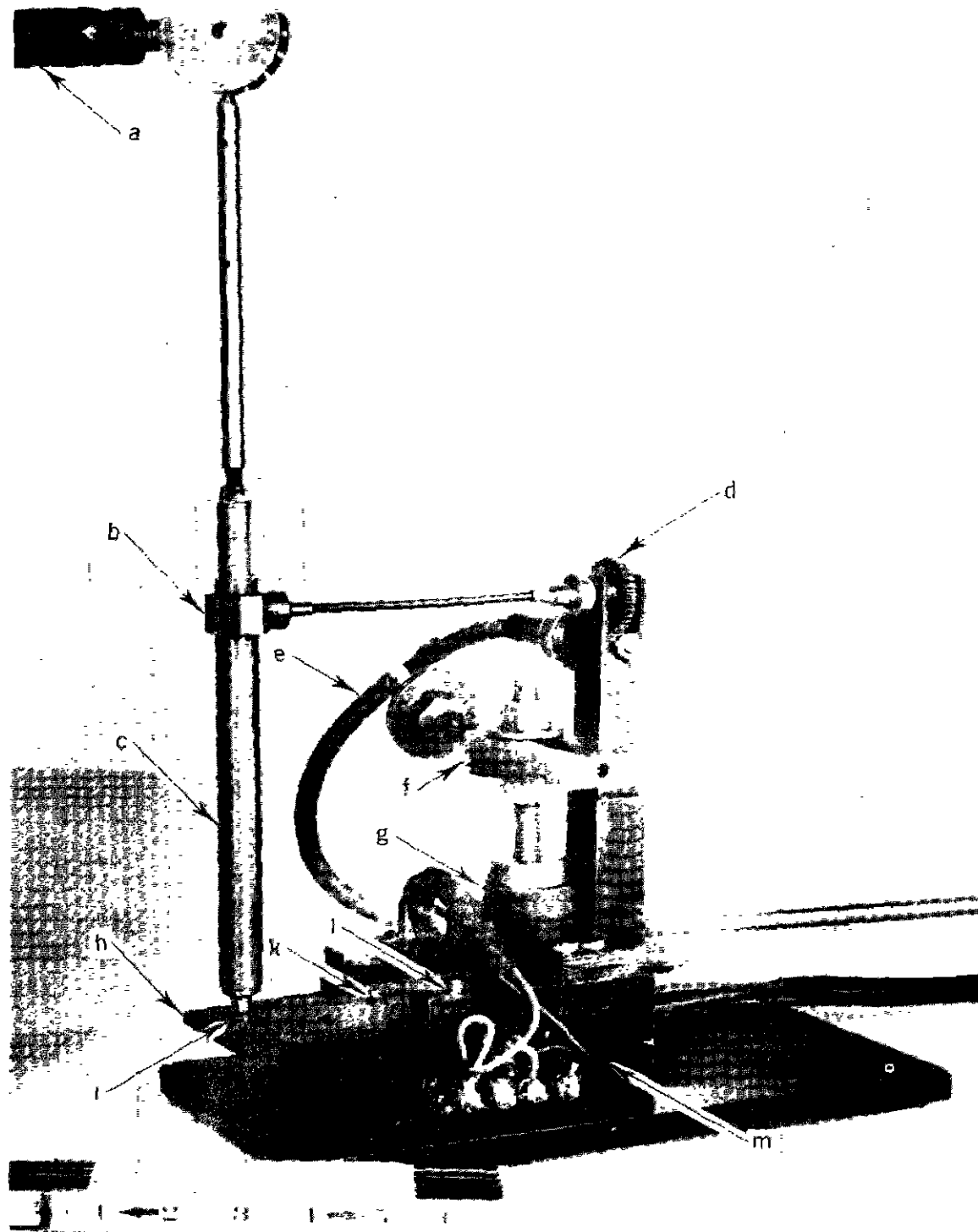


Figure 3 Phase Angle Versus Discord for Half Aperiodic Damping



- | | | | |
|---|---------------------|---|--|
| a | STRAIN GAGES | g | SPRING |
| b | STRAIN GAGE CARRIER | h | LOCK FOR e AND f |
| c | FRAME FOR b | i | WORM AND GEAR DRIVE |
| d | CONTACT POINTS | k | FLEXIBLE SHAFT FOR
REMOTE CONTROL |
| e | CYLINDER | l | CONNECTION TO HUB
OF AIRPLANE WHEEL |
| f | PISTON | | |

Figure 4 Diagram of Displacement Indicator with Two Reference Points



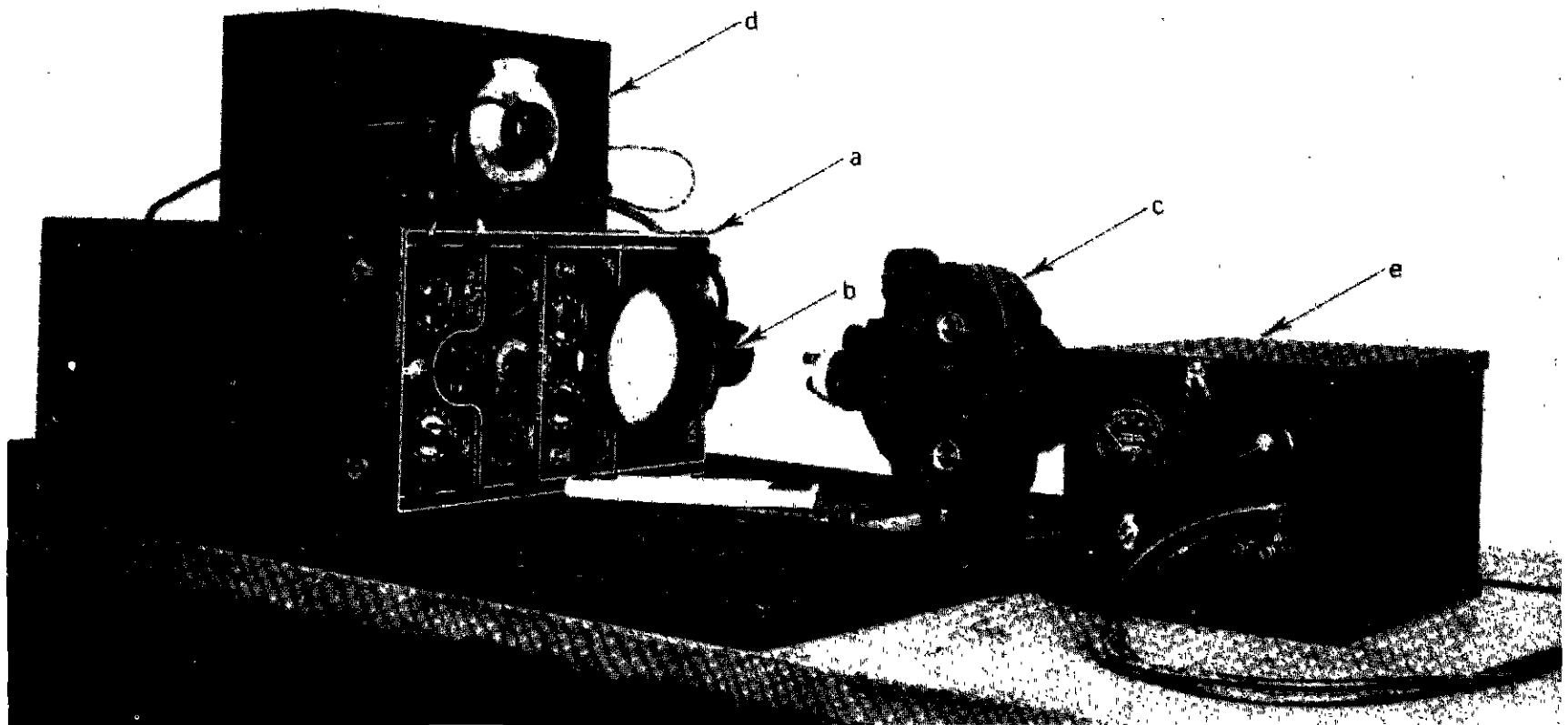
a CONNECTING ARM HUB OF AIRPLANE WHEEL
 b PISTON
 c CYLINDER
 d WORM AND GEAR DRIVE TO LOCK b AND c
 e FLEXIBLE CABLE

f HOLDING DOWN DEVICE FIXED TO WINDSHIELD
 g RUBBER INSULATOR BETWEEN f AND INDICATOR
 h STRAIN GAGE CARRIER
 i, k, l CONTACT POINTS ON h
 m STEEL FRAME FOR h AND d

Figure 5 Displacement Indicator with Two Reference Points



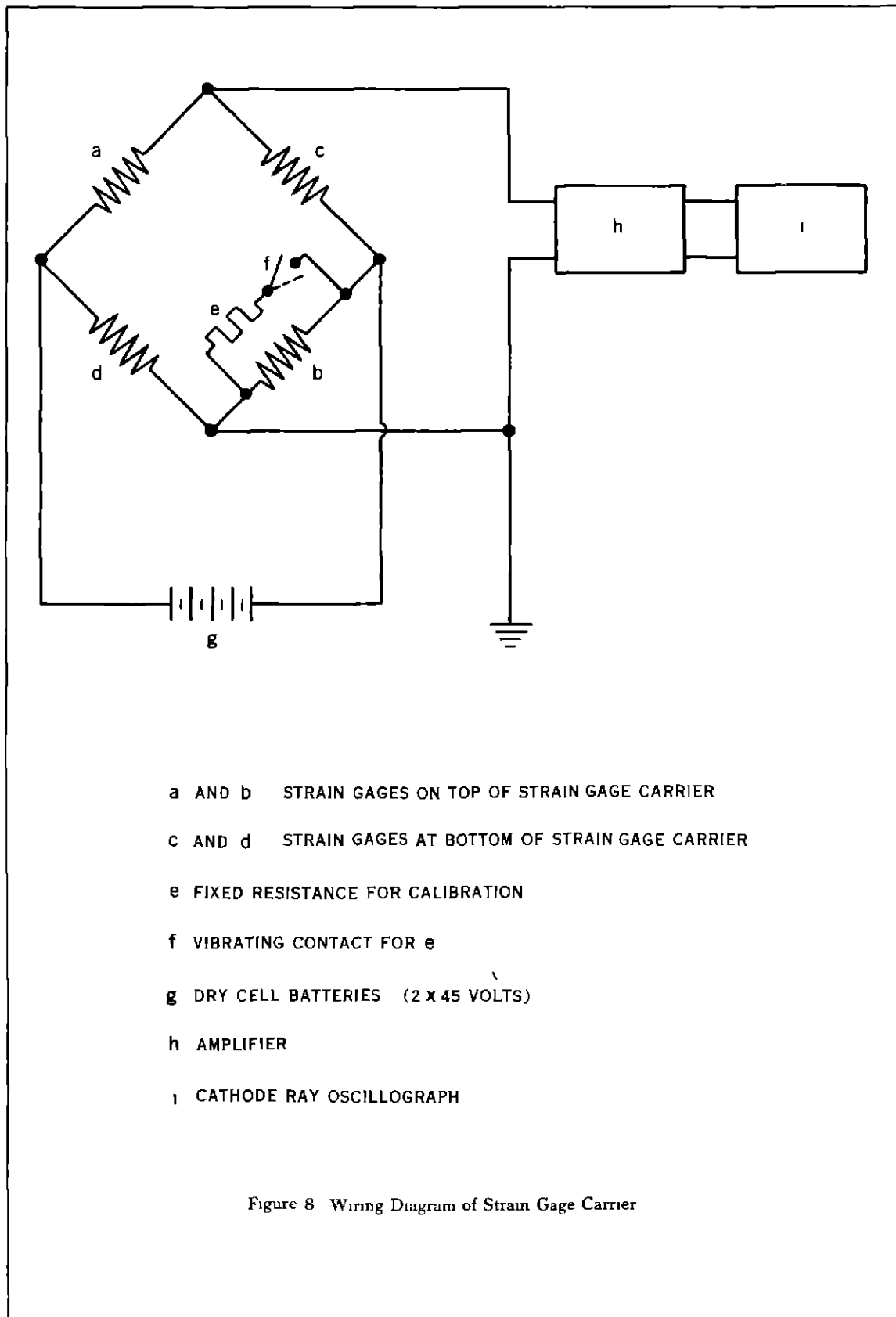
Figure 6 Displacement Indicator with Two Reference Points
Holding Down Device and Windshield Removed

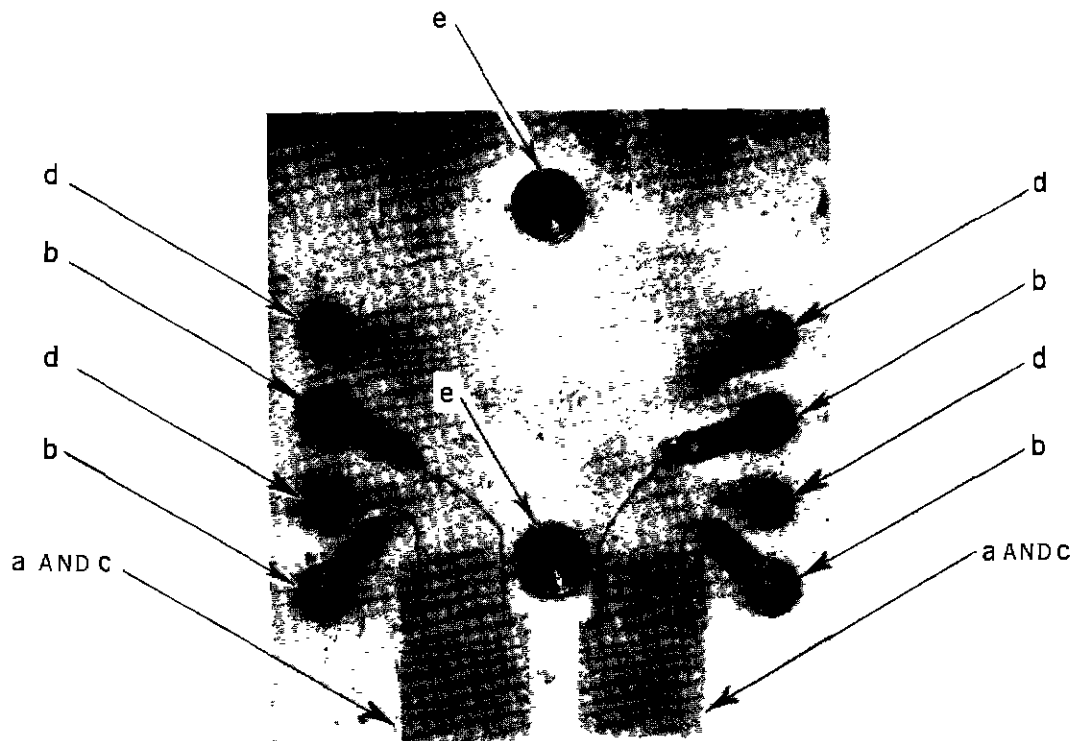


- a OSCILLOGRAPH
- b NEON LAMP FOR TIME SIGNAL
- c CAMERA

- d AMPLIFIER UNIT
- e BATTERY BOX

Figure 7 Auxiliary Equipment for Pick-Up Units
(Light Shield Between Camera and Oscillograph Removed)





- a STRAIN GAGES ON TOP OF LUCITE CARRIER
- b ELECTRIC CONTACTS FOR CONNECTIONS OF a
- c STRAIN GAGES AT BOTTOM LUCITE CARRIER
- d ELECTRIC CONTACTS FOR CONNECTIONS OF c
- e STEEL CONTACT POINTS FOR CONNECTING ROD TO HUB OF AIRPLANE WHEEL

Figure 9 Strain Gage Carrier for Displacement Indicator with Two Reference Points



NATURAL FREQUENCY 85 c p s

DAMPING $\epsilon = 1.131$, $\eta = 0.122$

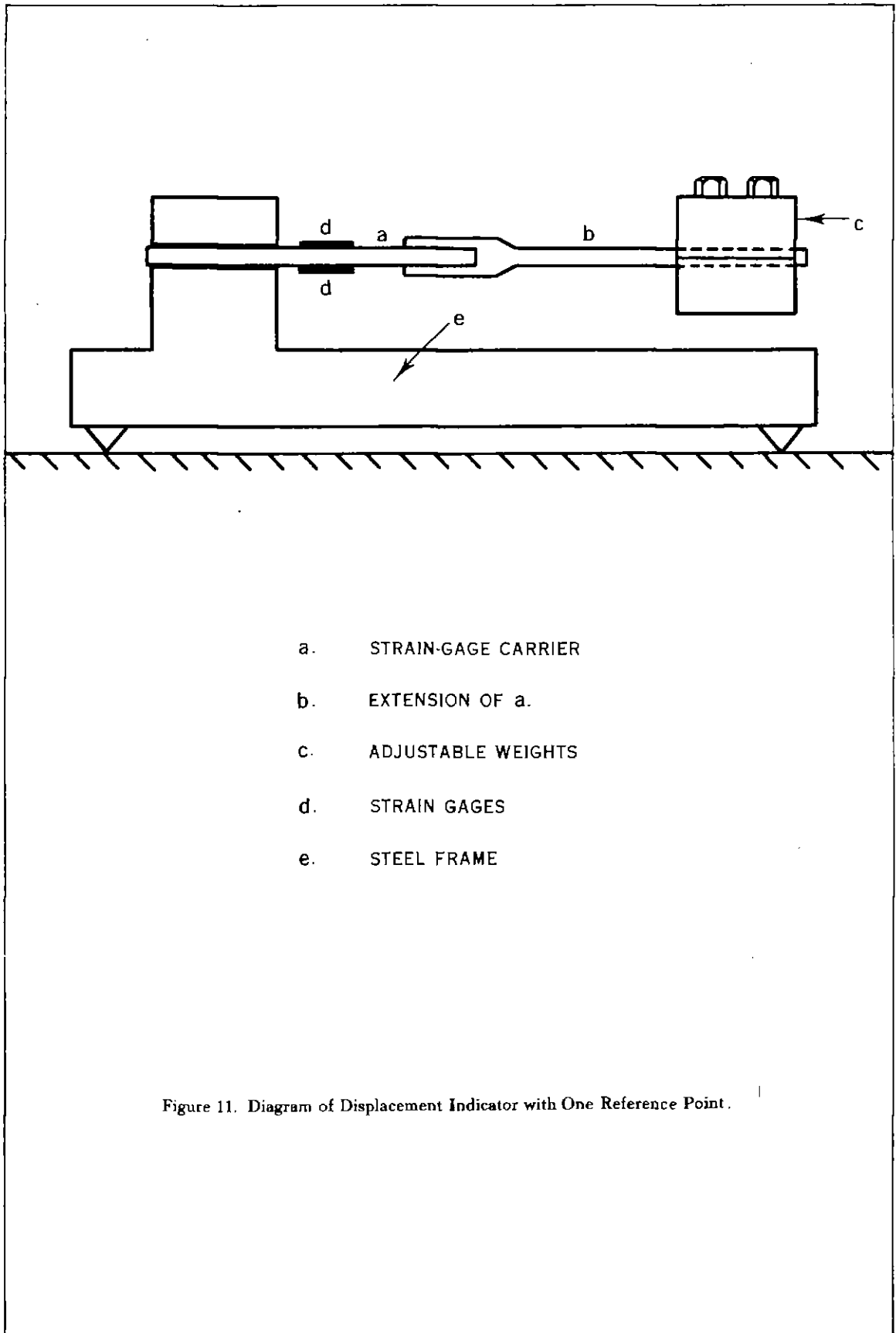
MAXIMUM DISPLACEMENT AMPLITUDE AT OUTER STEEL CONTACT POINT 0.05 INCH

MAXIMUM AMPLITUDE ON OSCILLOGRAPH SCREEN APPROX 2.5 INCHES

MAGNIFICATION ON OSCILLOGRAPH SCREEN 50X

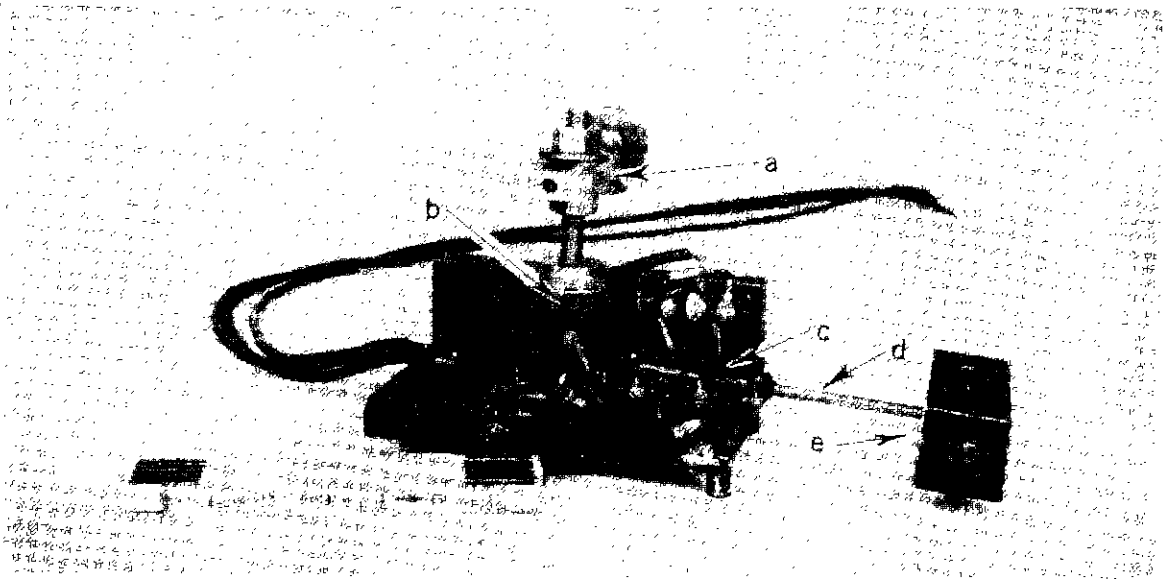
TIME SIGNAL 60 c p s

Figure 10 Determination of Natural Frequency of Displacement Indicator with Two Reference Points
(Strain Gage Carrier Alone) Record of Dying-Out Motion



- a. STRAIN-GAGE CARRIER
- b. EXTENSION OF a.
- c. ADJUSTABLE WEIGHTS
- d. STRAIN GAGES
- e. STEEL FRAME

Figure 11. Diagram of Displacement Indicator with One Reference Point.



- a. HOLDING DOWN DEVICE TO BE CONNECTED TO WINDSHIELD
- b. RUBBER DAMPER BETWEEN a. AND INDICATOR
- c. STRAIN GAGE CARRIER
- d. EXTENSION OF c.
- e. ADJUSTABLE WEIGHTS

Figure 12. Displacement Indicator with One Reference Point Set-Up for Vertical Motion.

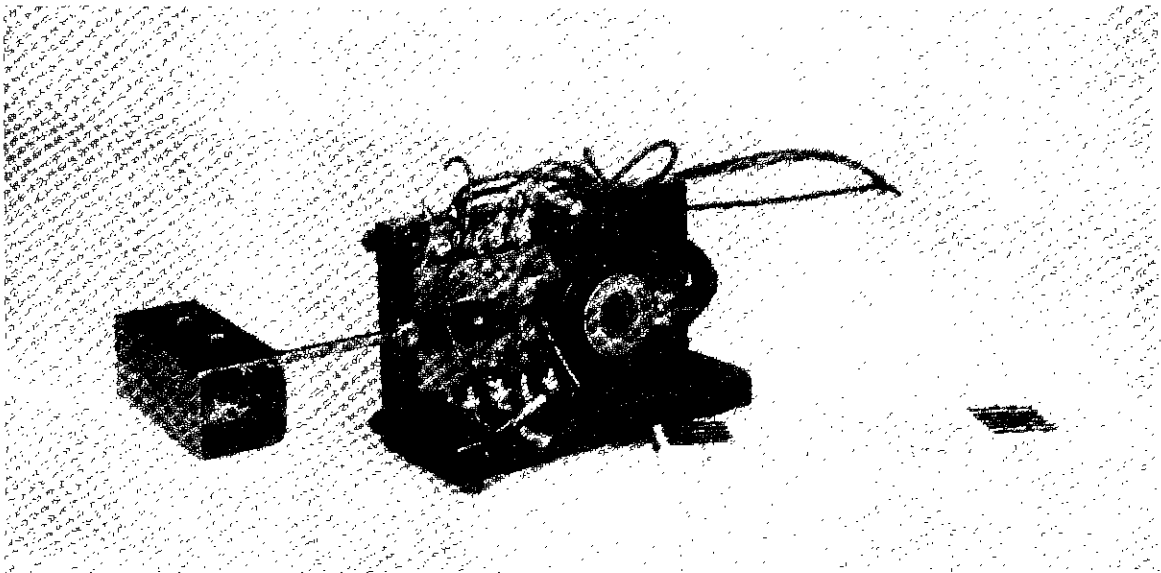
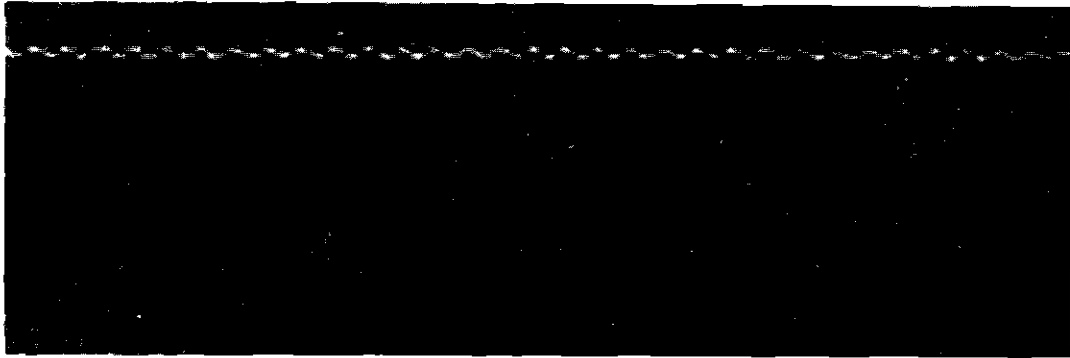


Figure 13. Displacement Indicator with One Reference Point Set-Up for Horizontal Motion.



NATURAL FREQUENCY 7 c p s

DAMPING $\epsilon = 1.41$ $\eta = 0.336$

MAXIMUM DISPLACEMENT AMPLITUDE AT FREE
END OF LUCITE CARRIER 0.05 INCH

MAXIMUM AMPLITUDE ON OSCILLOGRAPH
SCREEN 2.5 INCHES

MAGNIFICATION ON OSCILLOGRAPH SCREEN 50X

TIME SIGNAL 60 c p s

Figure 14 Determination of Natural Frequency and Damping of Displacement
Indicator with One Reference Point
Record of Dying-Out Motion

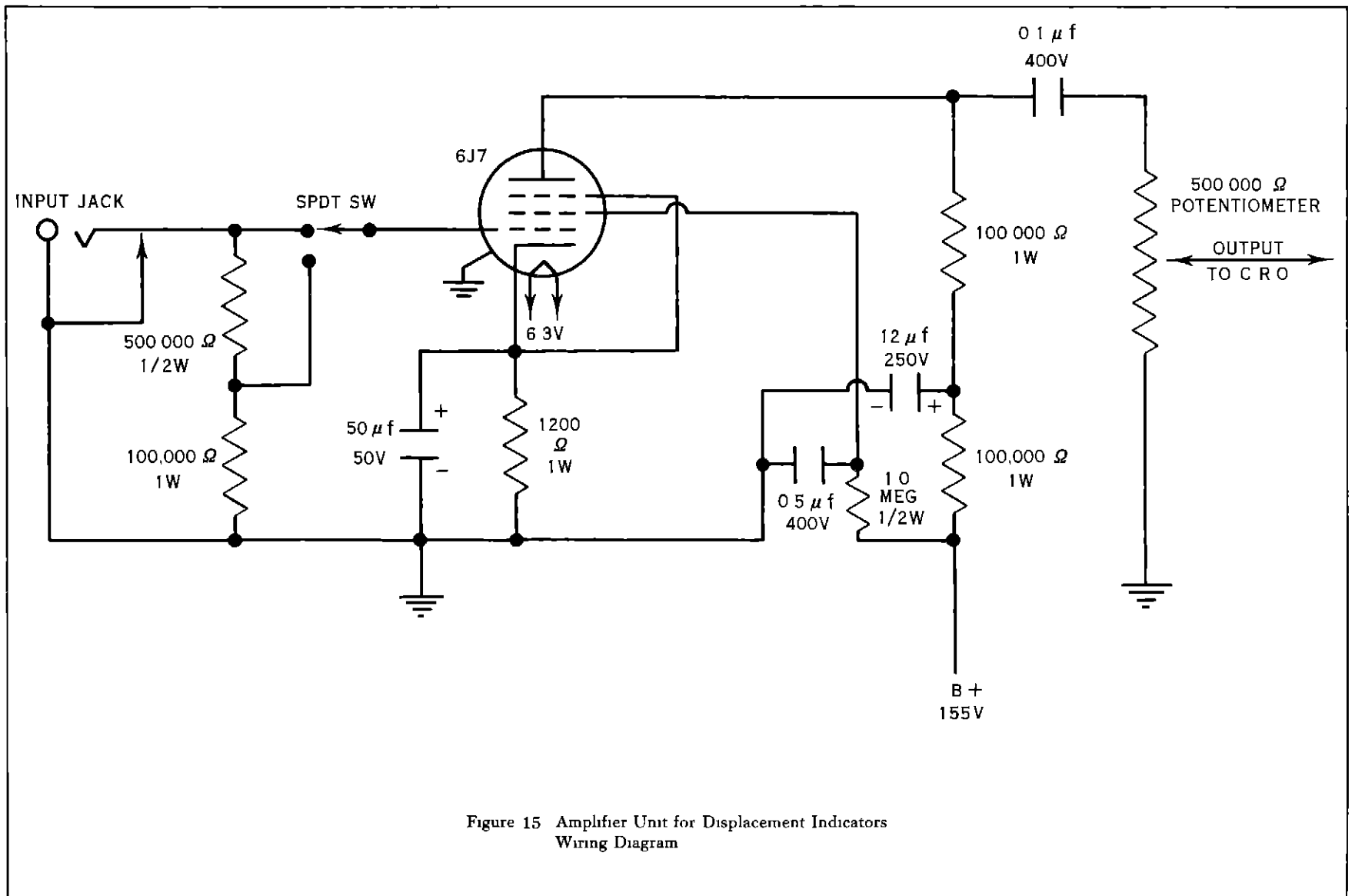


Figure 15 Amplifier Unit for Displacement Indicators
Wiring Diagram

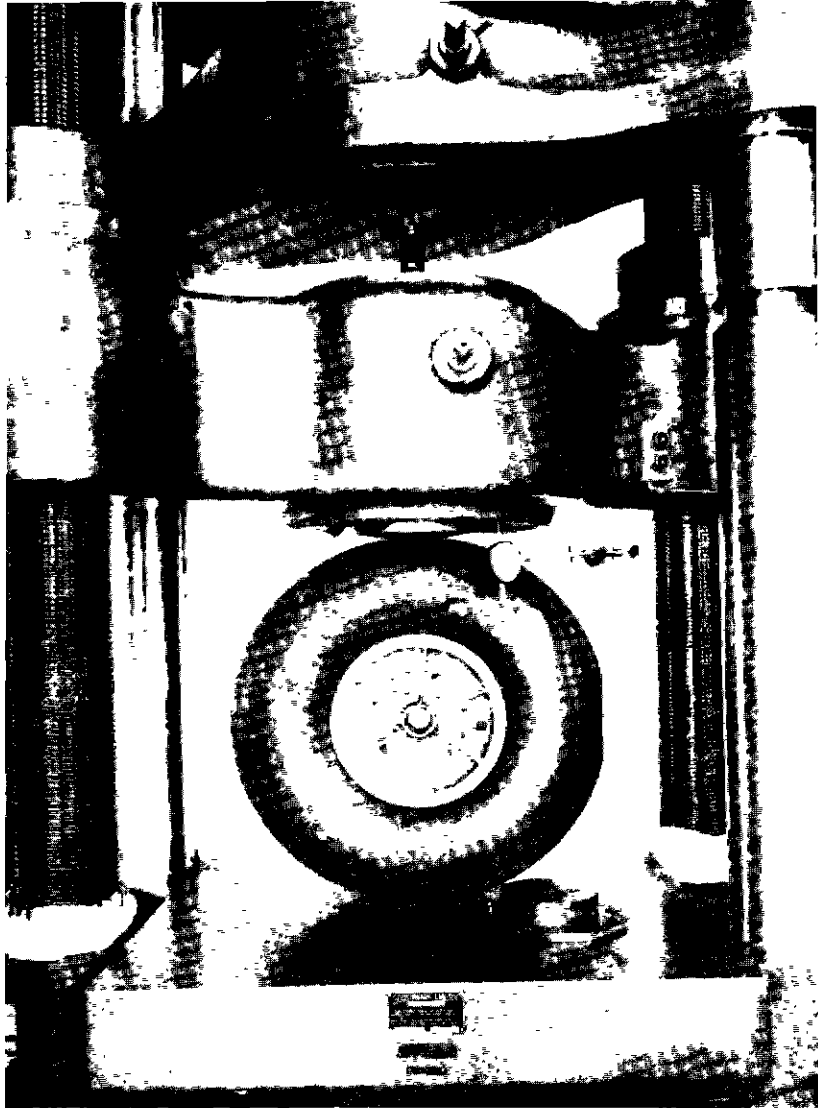


Figure 16 Static Calibration of Airplane Tire in 400,000 lb
Universal Testing Machine

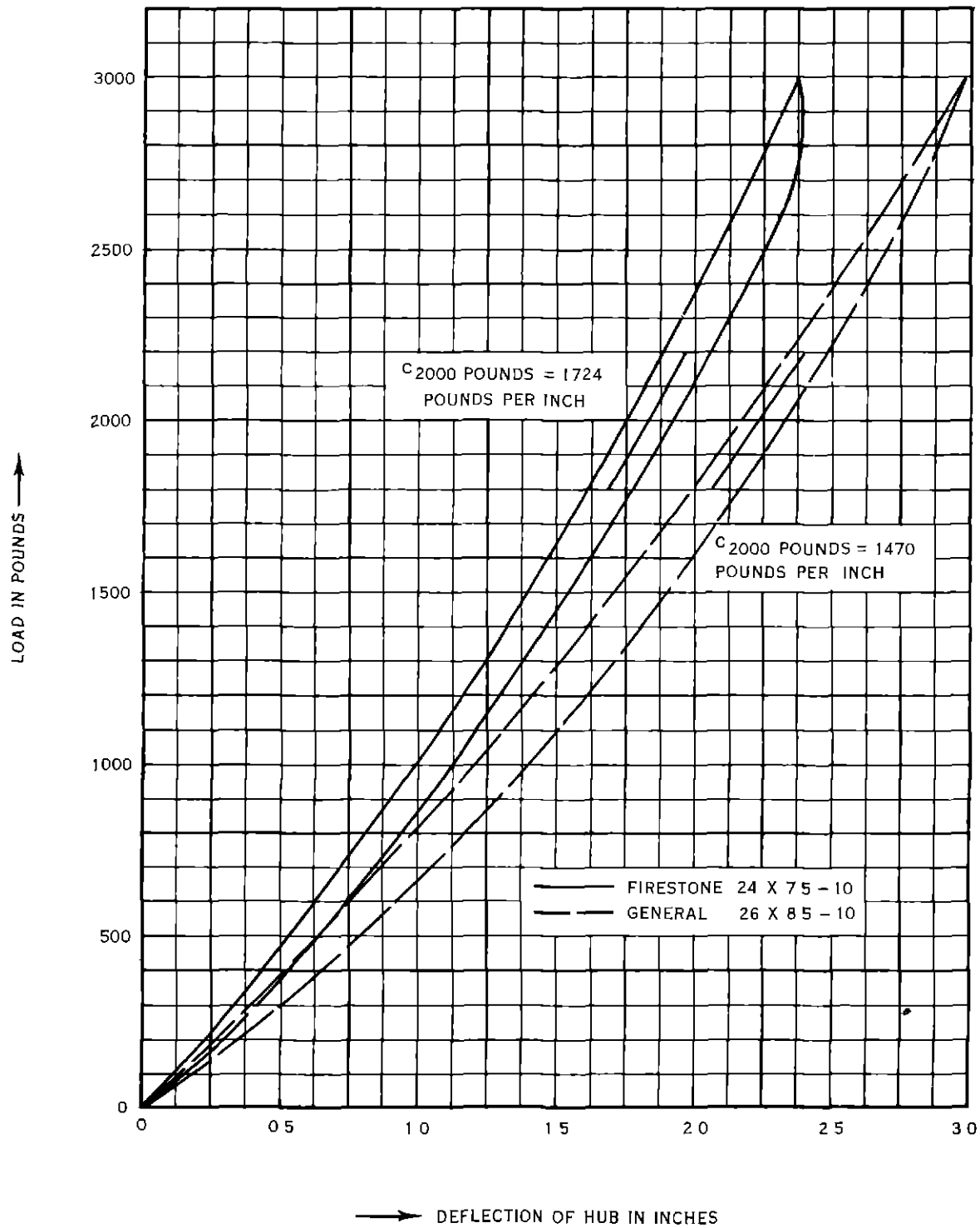


Figure 17 Static Deflection Load Diagram of Airplane Tires
Air Pressure 30 lb per sq in

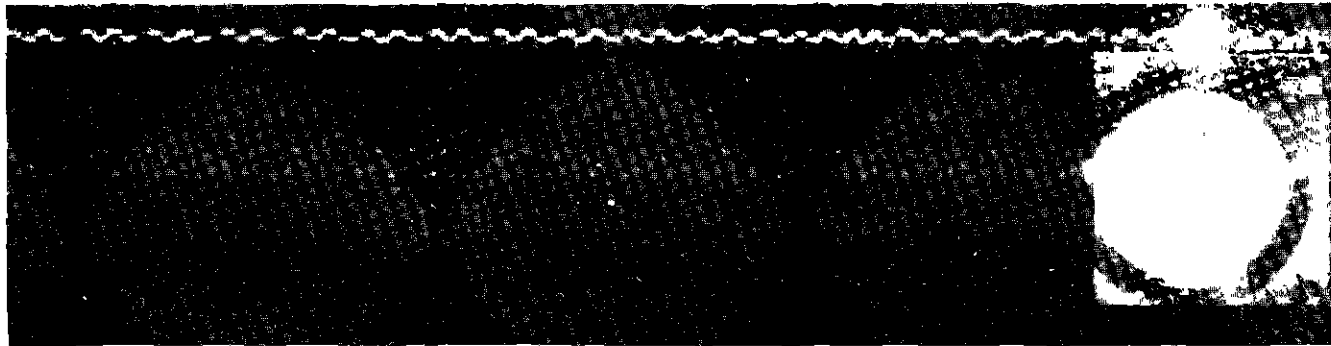


Figure 18 Imprint of Airplane Tire Under a Static Load of 2000 lb
Air Pressure 30 lb per sq in
Contact Pressure 36 lb per sq in

FREQUENCY 65 c p s
DOUBLE AMPLITUDE ON OSCILLOGRAPH SCREEN 0.9 INCH
ON TABLE 0.001 INCH

MAGNIFICATION ON OSCILLOGRAPH SCREEN 900X
TIME SIGNAL 60 c p s


Figure 19 Calibration of Displacement Indicator with Two Reference Points
Record of Sinusoidal Motion of Vibration Table



FREQUENCY 70 c p s
DOUBLE AMPLITUDE ON OSCILLOGRAPH SCREEN 0.8 INCH
ON TABLE 0.001 INCH

MAGNIFICATION ON OSCILLOGRAPH SCREEN 800X
TIME SIGNAL 60 c p s

Figure 20 Calibration of Displacement Indicator with Two Reference Points
Record of Sinusoidal Motion of Vibration Table



FREQUENCY 160 c p s
DOUBLE AMPLITUDE ON OSCILLOGRAPH SCREEN 0.7 INCH
ON TABLE 0.001 INCH

MAGNIFICATION ON OSCILLOGRAPH SCREEN 700X
TIME SIGNAL 60 c p s

Figure 21 Calibration of Displacement Indicator with Two Reference Points
Record of Sinusoidal Motion of Vibration Table

FREQUENCY 65 c p s
DOUBLE AMPLITUDE ON OSCILLOGRAPH SCREEN 2.5 INCHES
ON TABLE 0.001 INCH

MAGNIFICATION ON OSCILLOGRAPH SCREEN 2500X
TIME SIGNAL 60 c p s

Figure 22 Calibration of Displacement Indicator with One Reference Point
Record of Sinusoidal Motion of Vibration Table



FREQUENCY 70 c p s

DOUBLE AMPLITUDE ON OSCILLOGRAPH SCREEN 3 INCHES
ON TABLE 0 001 INCH

MAGNIFICATION ON OSCILLOGRAPH SCREEN 3000X

TIME SIGNAL 60 c p s

Figure 23 Calibration of Displacement Indicator with One Reference Point
Record of Sinusoidal Motion of Vibration Table

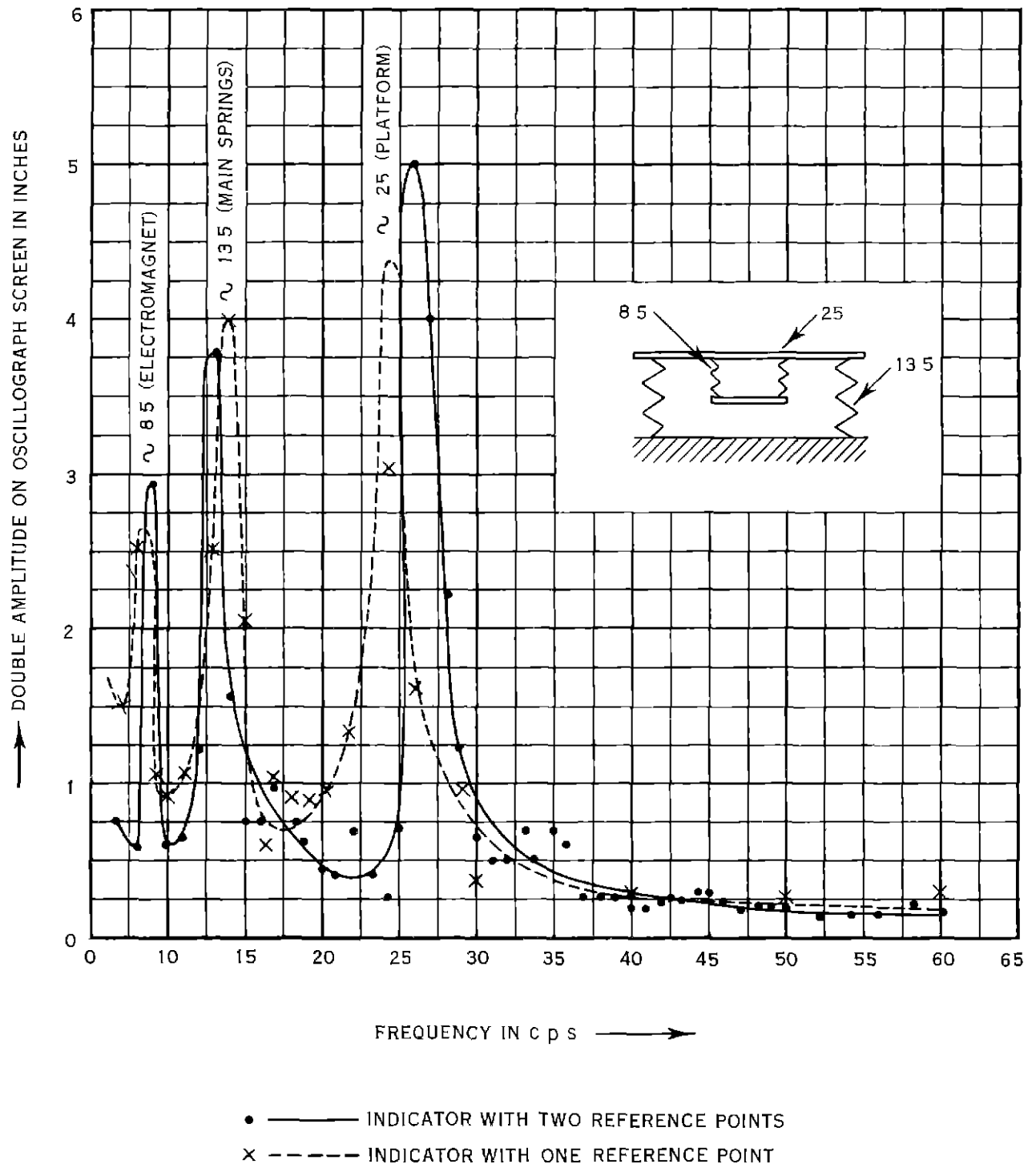
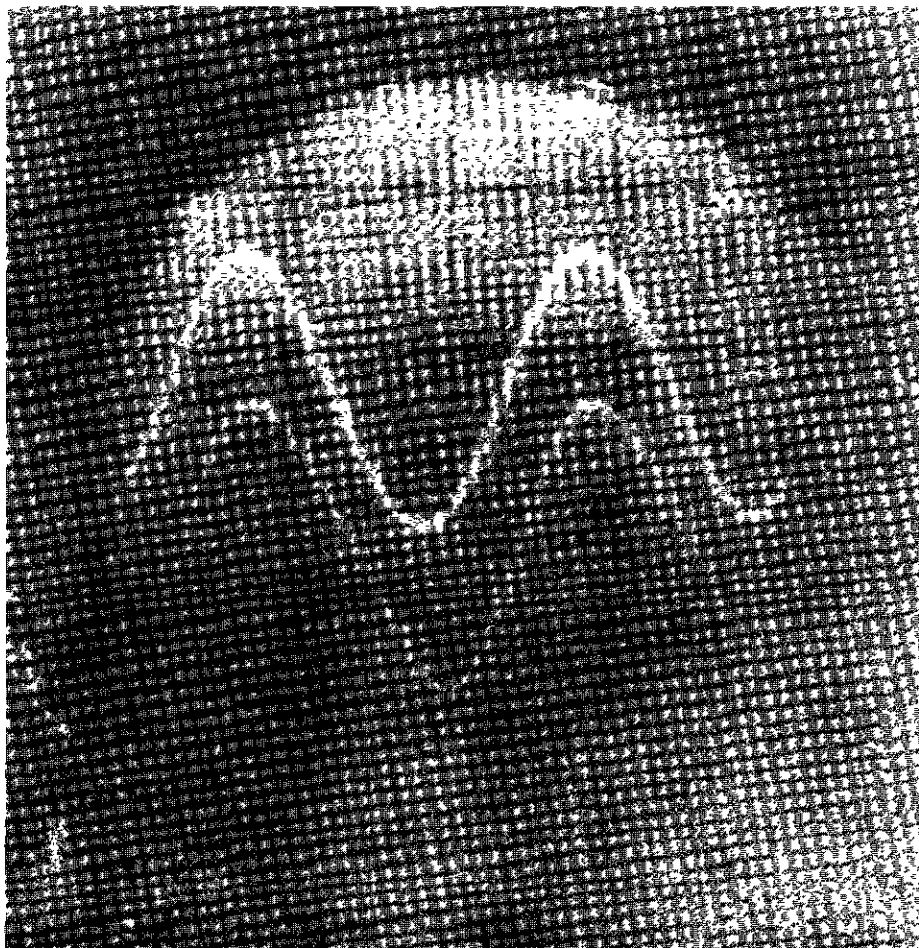


Figure 24 Calibration of Displacement Indicators
 Frequency Spectrum of Vibration Table from 7 to 60 cps



FREQUENCY 50 c p s

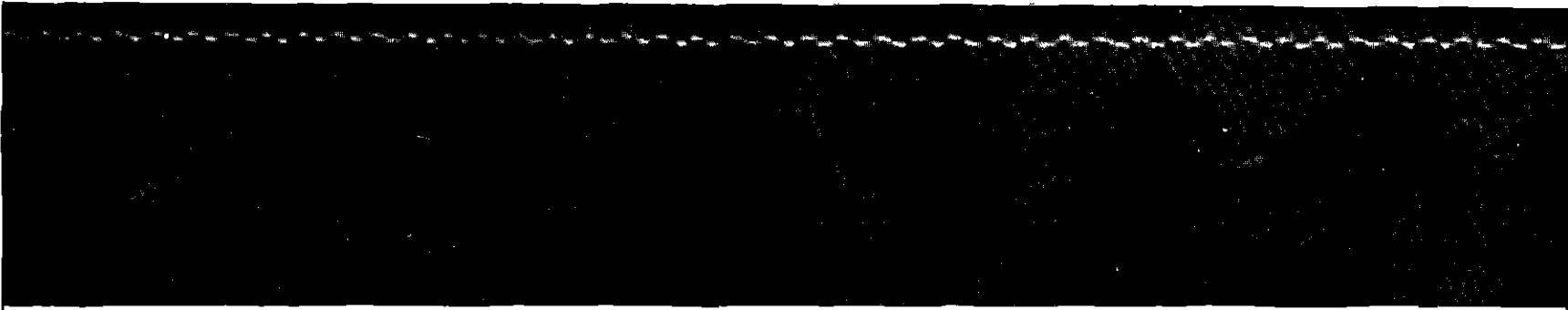
DOUBLE AMPLITUDE ON OSCILLOGRAPH SCREEN 1.7 INCH
ON TABLE 0.001 INCH

MAGNIFICATION ON OSCILLOGRAPH SCREEN 1700X

Figure 25 Calibration of Displacement Indicators
Sinusoidal Motion of Vibration Table Recorded Simultaneously
with Both Instruments by Means of an Electronic Switch



Figure 26 Calibration of Displacement Indicators Record of Hysteresis
Loop of a Rubber Damper
X-Axis Effect of Damping Action
Y Axis Effect of Elastic Action
Phase Angle $14^{\circ}20'$



IMPACT FREQUENCY APPROX 3 c p s

NATURAL FREQUENCY OF VIBRATION TABLE PLATFORM (MAIN SPRINGS
IN RESONANCE) APPROX 13

MAXIMUM DOUBLE AMPLITUDE ON OSCILLOGRAPH SCREEN 2.5 INCHES
ON TABLE APPROX 0.0005 INCH

MAGNIFICATION ON OSCILLOGRAPH SCREEN 5000X

TIME SIGNAL 60 c p s

Figure 27 Calibration of Displacement Indicator with Two Reference Points
Record of Nonperiodic Motion of Vibration Table

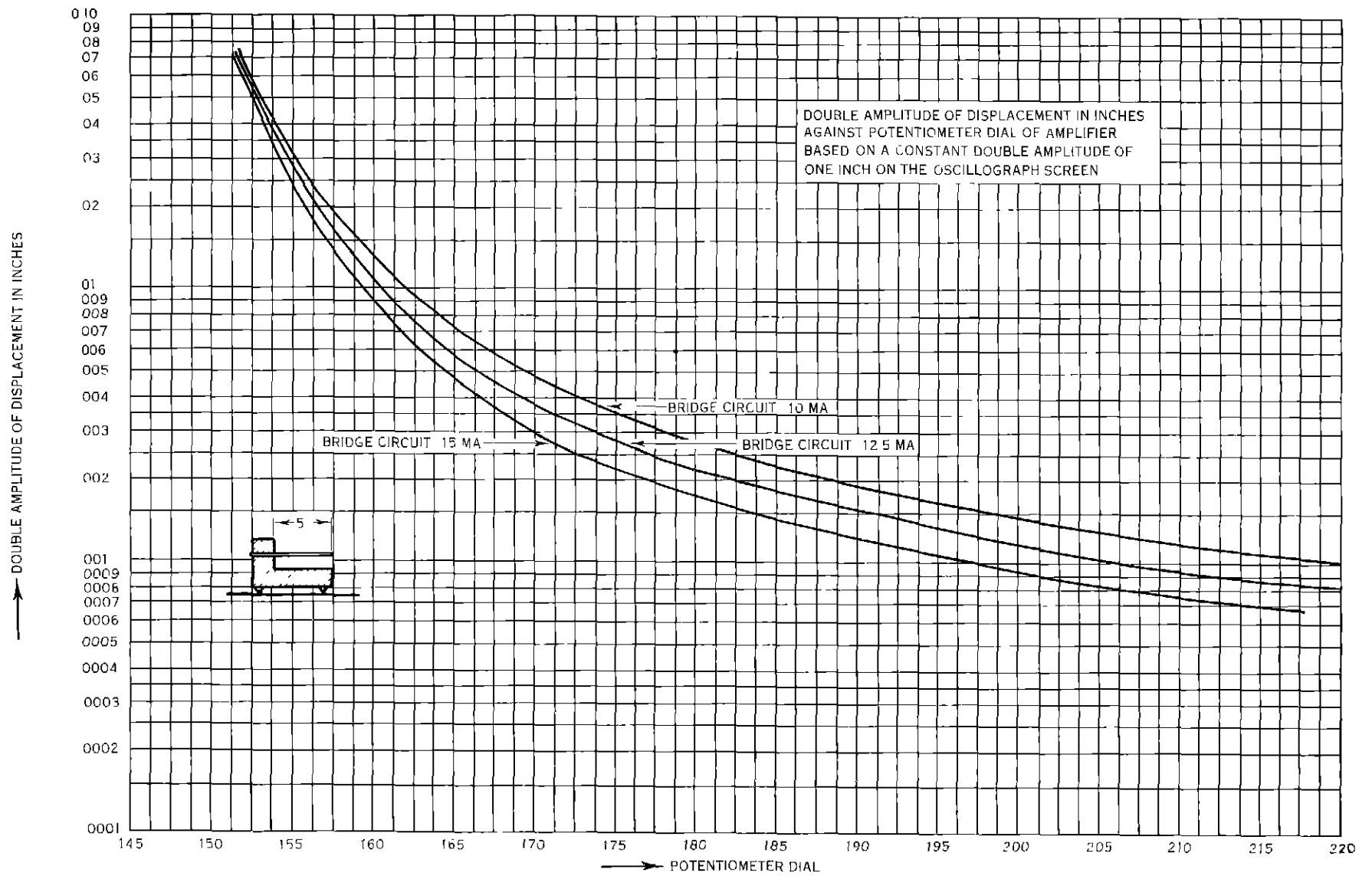


Figure 28 Calibration Curves for Displacement Indicator with Two Reference Points

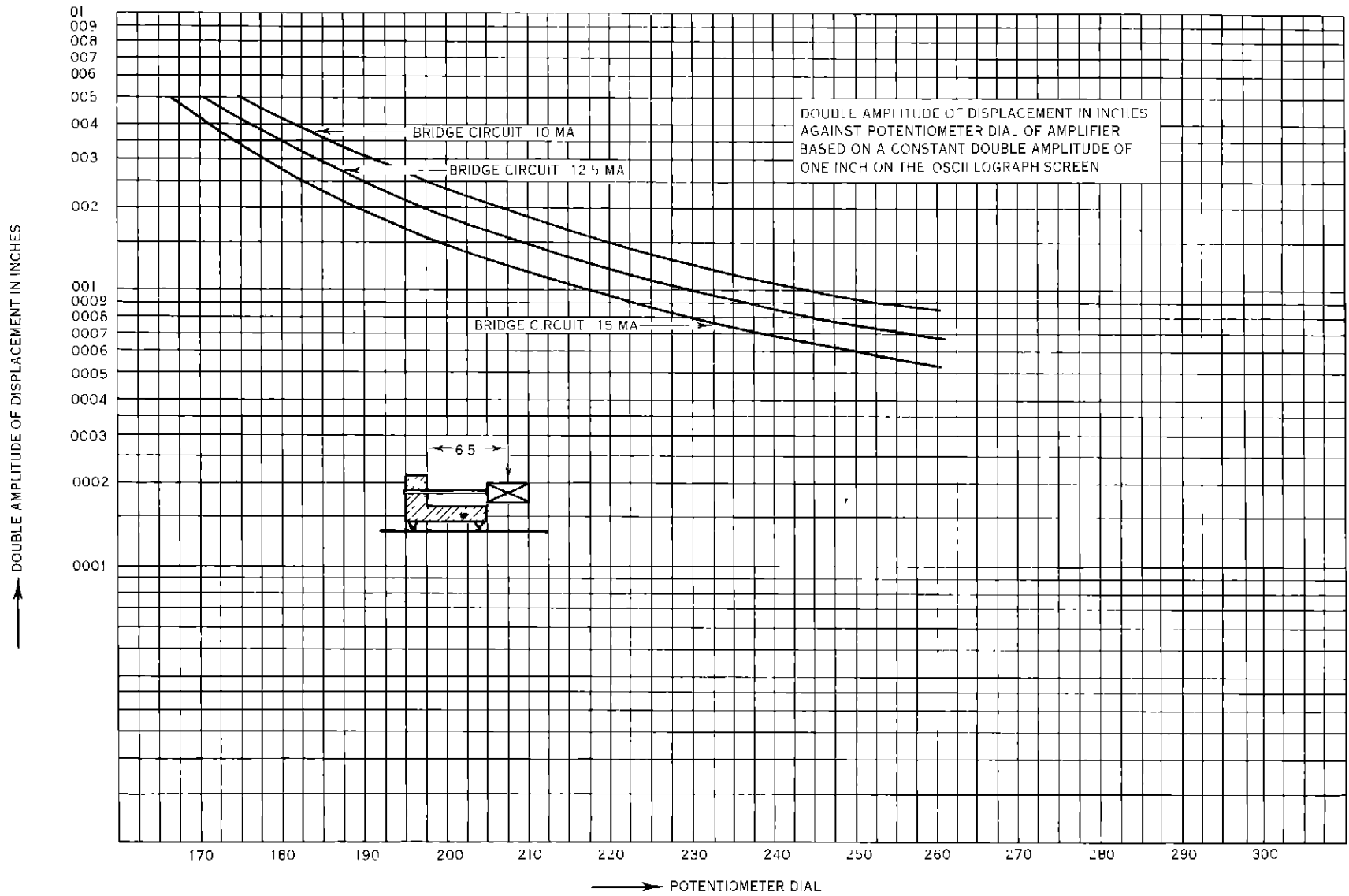


Figure 29 Calibration Curves for Displacement Indicator with One Reference Point

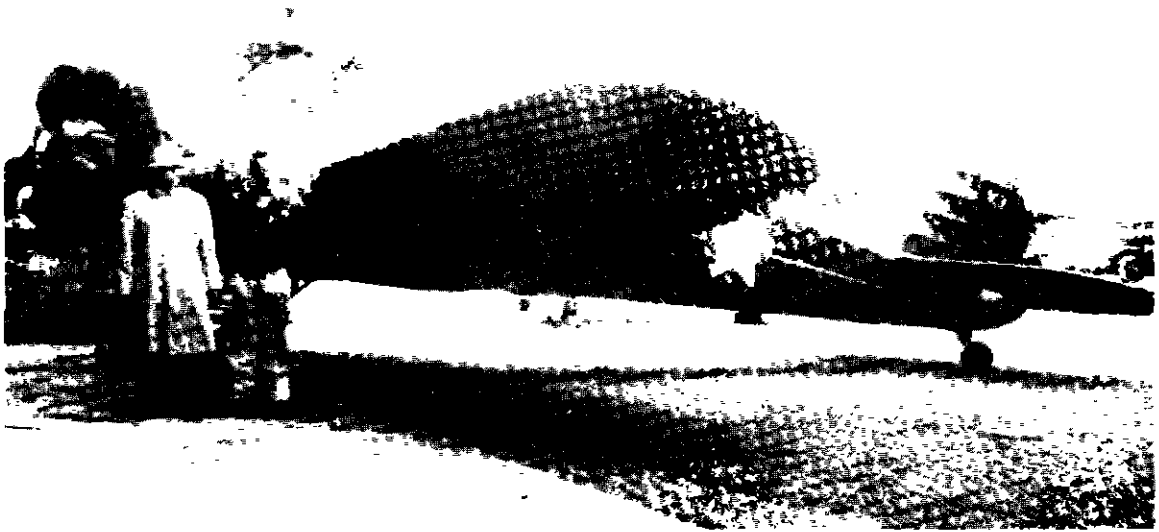


Figure 30 Cessna Plane on Apron Before the Regional Depot at La Guardia Field (New York, N Y) Side View

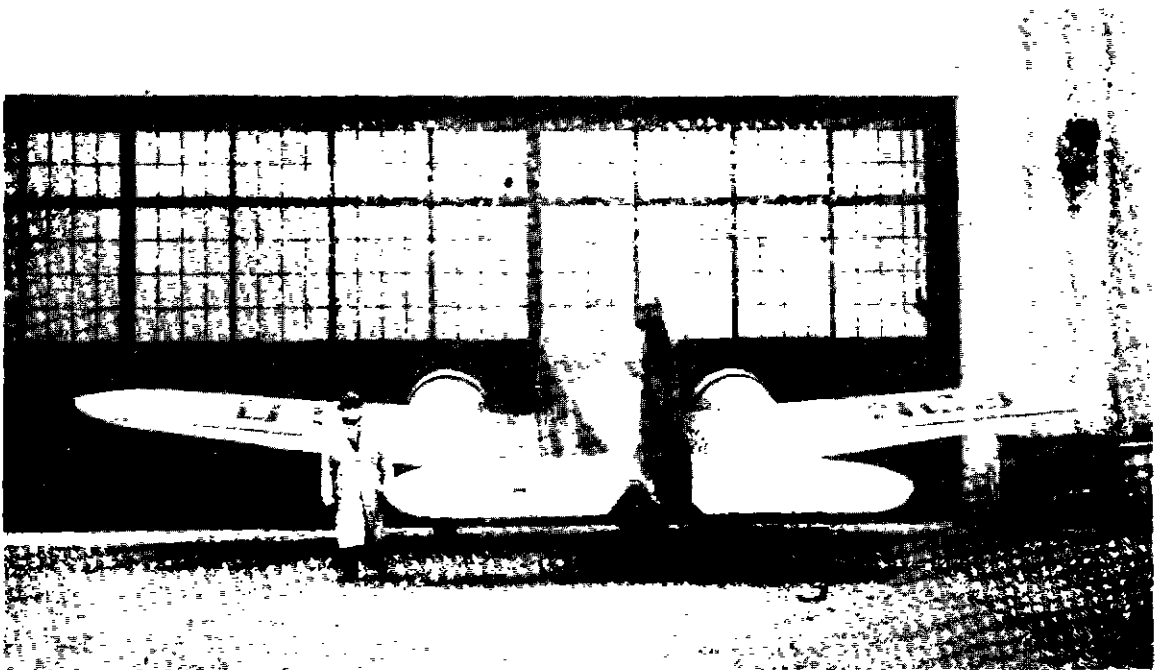


Figure 31 Cessna Plane on Apron Before the Regional Depot at La Guardia Field (New York, N Y) Rear View

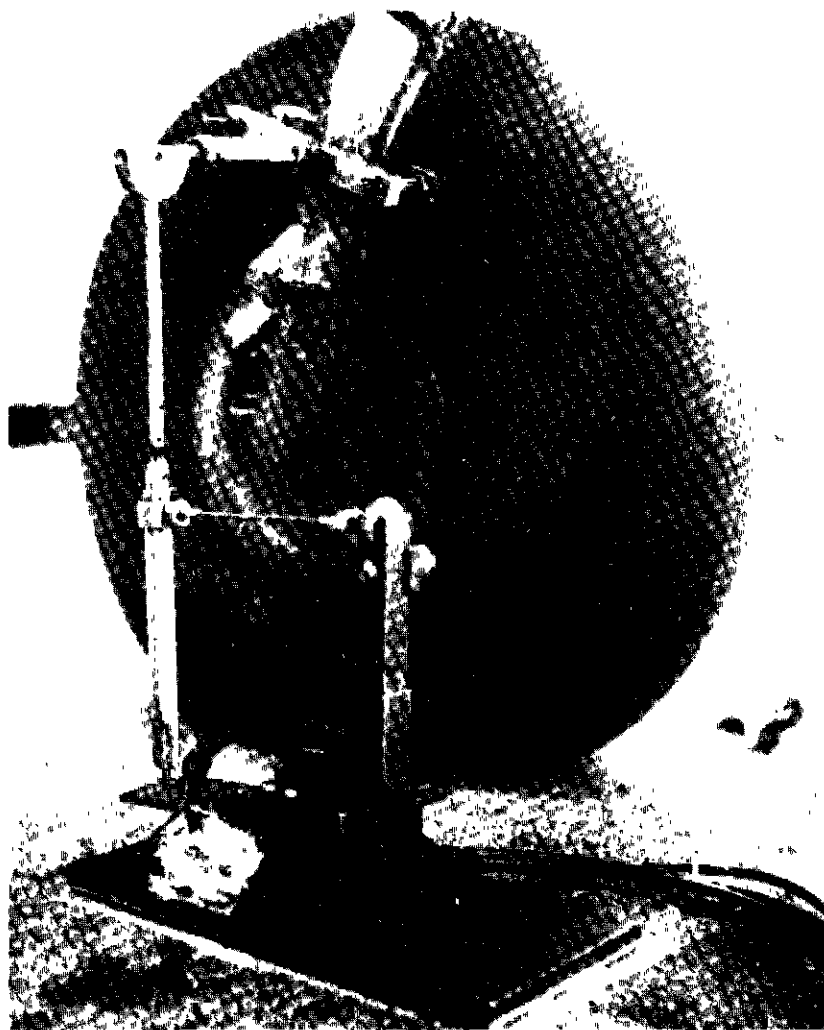


Figure 32 Indicator with Two Reference Points Connected to Airplane Wheel (Windshield Removed) Side View

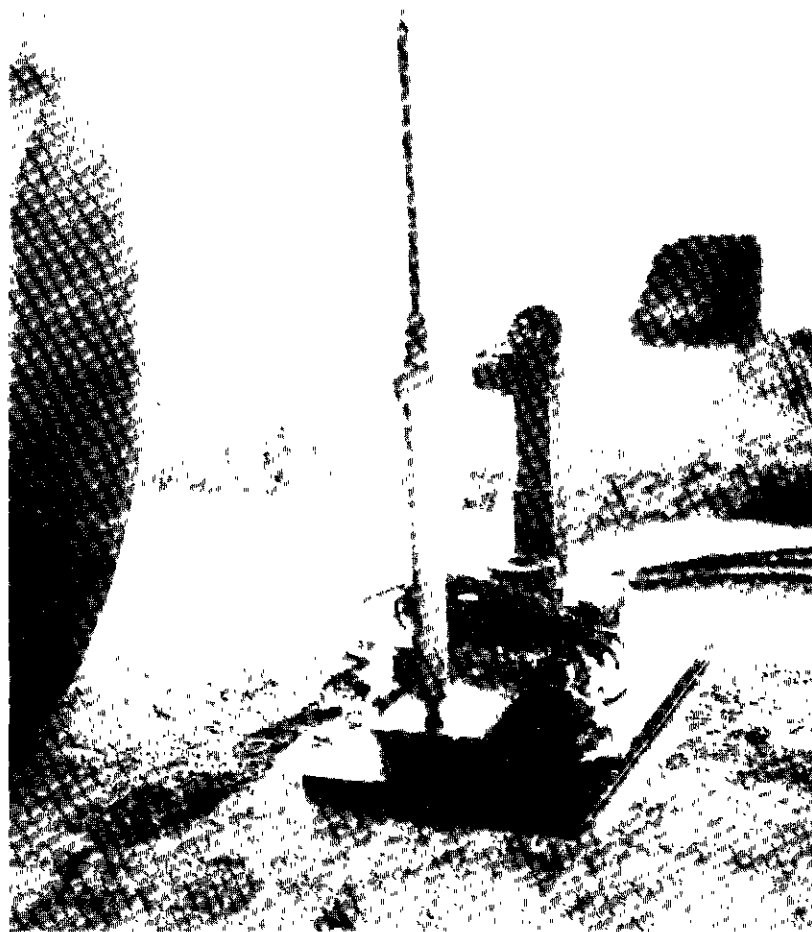


Figure 33 Indicator with Two Reference Points Connected to Airplane Wheel (Windshield Removed) Rear View

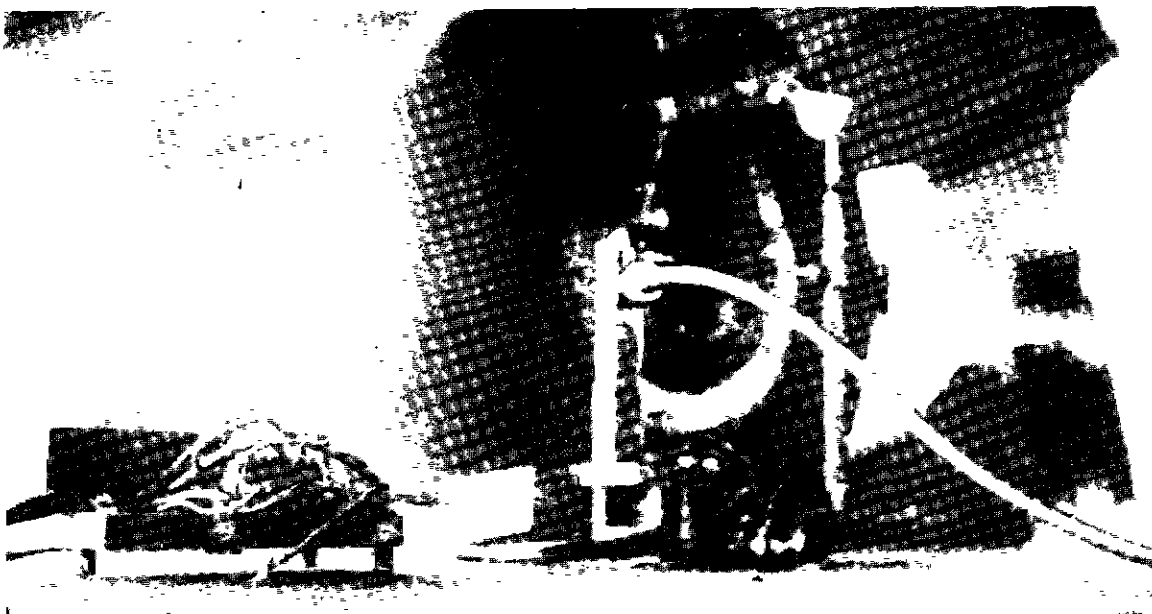


Figure 34 Indicator with Two Reference Points and with One Reference Point (Windshield Removed) Side View

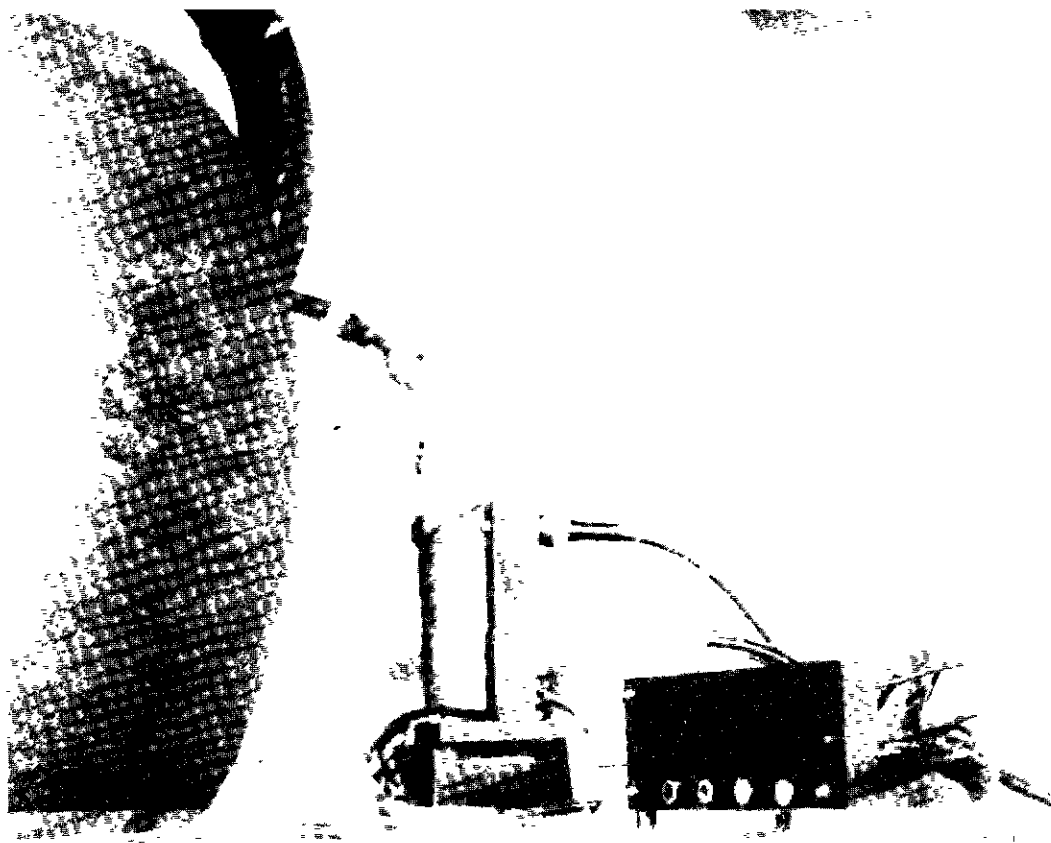


Figure 35 Indicator with Two Reference Points and with One Reference Point (Windshield Removed) Rear View



Figure 36 Windshield and Airplane Wheel Front View

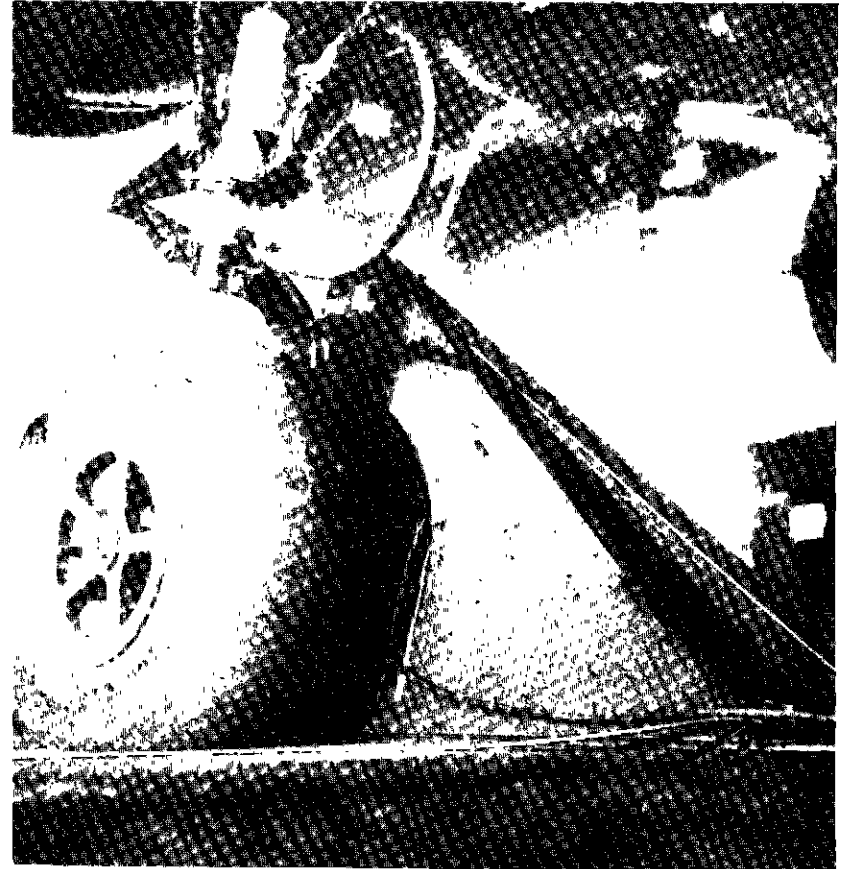
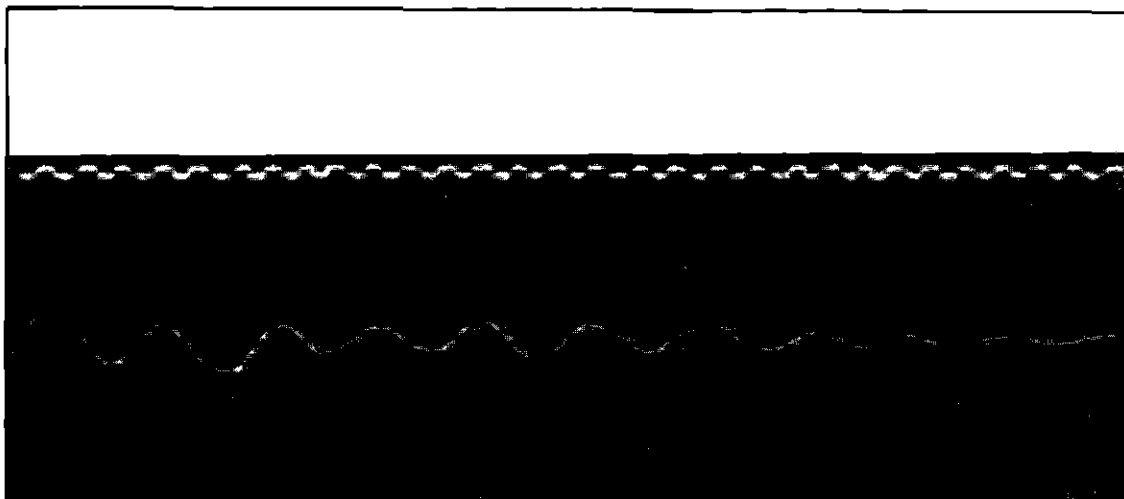


Figure 37 Windshield and Airplane Wheel Side View



DYING OUT FREQUENCY APPROX 20 c p s

EXCITER FORCE FREQUENCY APPROX 15 c p s

DAMPING $\epsilon = 1.25$, $\eta = 0.233$

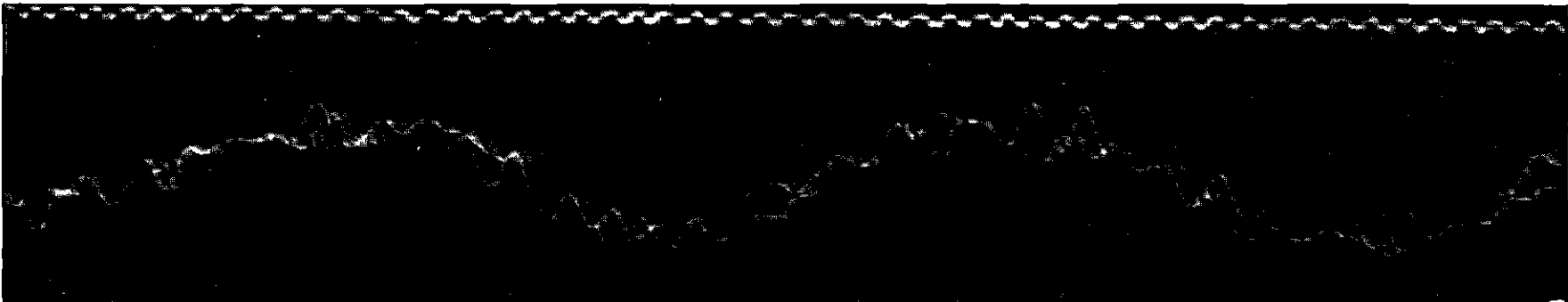
MAXIMUM DOUBLE DISPLACEMENT AMPLITUDE (HUB-PAVEMENT) 0.0013 INCH
ON OSCILLOGRAPH SCREEN 1.8 INCHES

MAGNIFICATION ON OSCILLOGRAPH SCREEN 1380X

MAXIMUM FORCE AMPLITUDE (TIRE PAVEMENT) APPROX ± 1 LB

TIME SIGNAL 60 c p s

Figure 38 Record of Displacement Indicator with Two Reference Points
Dying Out Motion Between Hub of Airplane Wheel and Pavement
Caused by an Intermittent Force Applied at the End of One Wing



RIGHT PROPELLER HIGH PITCH

LEFT PROPELLER IDLING

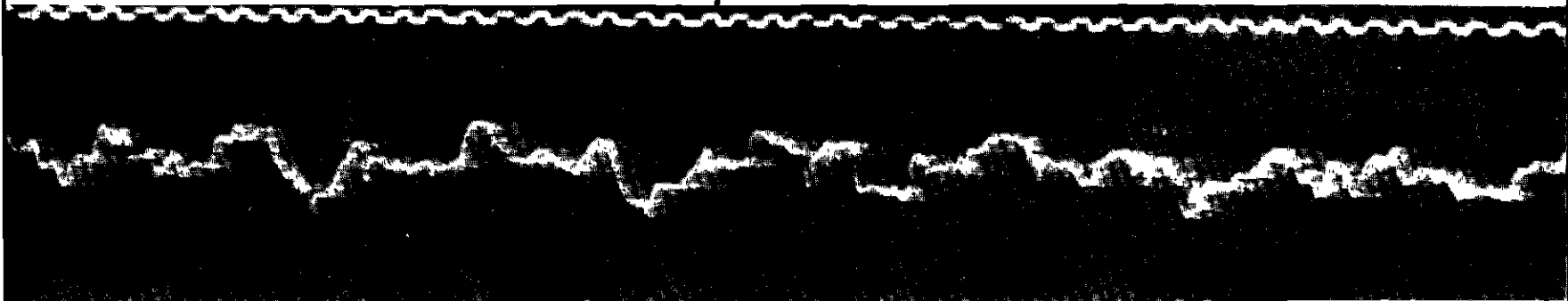
MAXIMUM FORCE AMPLITUDE (TIRE PAVEMENT) ± 22 LB

FREQUENCIES $n_1 = 3$ c p s

$n_2 =$ APPROX 50 c p s

REDUCED TIME SIGNAL APPROX 75 c p s

Figure 39 Record of Displacement Indicator with Two Reference Points
Motion Between Hub of Airplane Wheel and Pavement
Frequency Spectrum for Propeller Velocities Around 1,000 r p m



RIGHT PROPELLER 1200 r p m , HIGH PITCH

LEFT PROPELLER IDLING

MAXIMUM DISPLACEMENT AMPLITUDE OF PAVEMENT ± 0.002 INCH

FREQUENCIES $n_1 =$ APPROX 15 c p s

$n_2 =$ APPROX 50 c p s

TIME SIGNAL 60 c p s

Figure 40 Record of Displacement Indicator with One Reference Point
Motion of Pavement

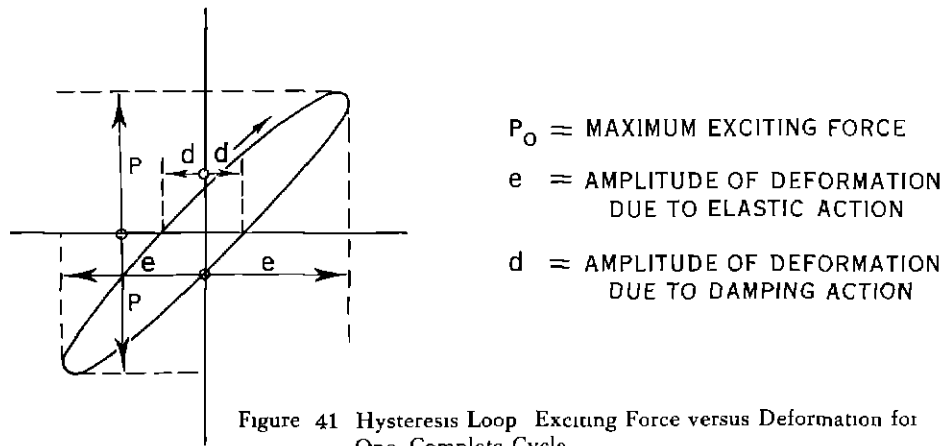


Figure 41 Hysteresis Loop Exciting Force versus Deformation for One Complete Cycle

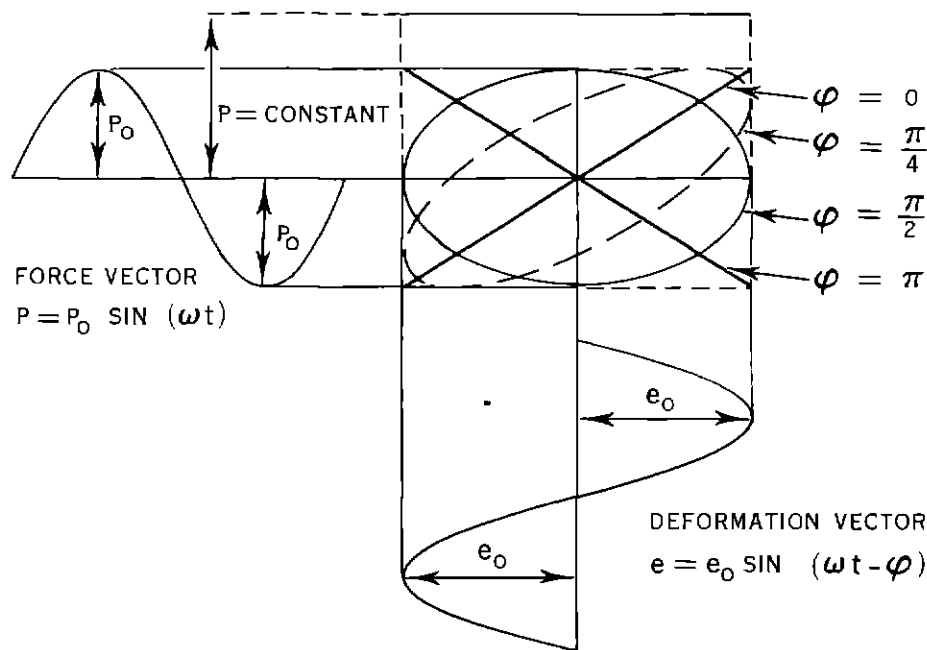


Figure 42 Relation Between Phase Angle (φ) and Form of Hysteresis Loop for Sinusoidal Vibrations

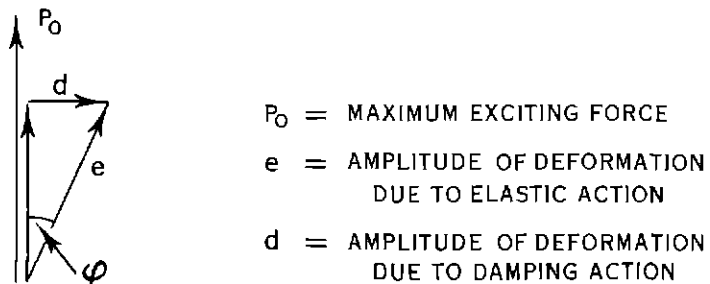


Figure 43 Relation Between Phase Angle (φ) and Force Vector (P)